

B.TECH PROJECT - STAGE I REPORT

Lorentzian OPE Inversion Formula

Amey P Gaikwad
Indian Institute of Technology, Bombay

Supervisors:
Dr. Shiraz Minwalla (TIFR, Mumbai)
Dr. Urjit Yajnik (IIT Bombay)

November 2018

Abstract

Any conformal field theory can be described using the fixed conformal data - the coefficient f_{ijk} appearing with the three point function and C_J accompanying the two point function of spinning operators. Given this conformal data any n -point function in a conformal field theory can be determined (by the OPE expansion). Now, this data varies from model to model and hence depends on the type of CFT we are dealing with. What we wish to understand is how to get this data from the knowledge of the correlators themselves. 4 point correlators should suffice as they impose strict constraints like crossing symmetry on the theory which can help us in our quest. Simon Caron-Huot came with this formalism the first time when he was successfully able to extract the CFT data by integrating the four point function over some region of Lorentzian spacetime. Stanford, Witten and Simmons-Duffin came up with another derivation of the same formula, but with a Wick rotation in spacetime rather than in the cross-ratio space. In this review, we wish to understand the physical content of this method; the connections between the two derivations and how exactly a mathematically abstract concept gives rise to physical CFT data.

Contents

1	Introduction	3
2	Conformal Field Theories	7
2.1	Definition	7
2.2	Operators and Correlators	8
2.2.1	Operators	8
2.2.2	Correlators	9
2.3	The Operator Product Expansion (OPE)	10
2.3.1	Primaries and descendants	10
2.3.2	Operator Product Expansion	11
2.4	Shadow formalism	12
2.5	Principal Series representation	13
3	Spacetime derivation	15
3.1	Introduction	15
3.2	2 dimensions	16
3.2.1	Euclidean Inversion formula	16
3.2.2	Wick rotation	18
3.2.3	The final formula	22
3.3	Higher dimensions	23
3.3.1	Euclidean inversion formula	23
3.3.2	Resolving the divergences	24
3.3.3	Wick rotation	25
3.3.4	In cross ratio terms	26
3.3.5	Evaluating the hanging integral	28
3.3.6	Integral over cross ratios	29
3.3.7	Analytic continuation in cross-ratio space	30
4	Cross-Ratio Derivation	35
4.1	Introduction	35
4.2	Inverting the formula	36
4.3	Wick rotation	38
4.3.1	Double Discontinuity	38
4.3.2	The Monodromies	39
4.3.3	Analytic Continuation	41
4.4	Comparing spacetime derivation and Cross ratio derivation	49
5	Conclusion	51

6	Acknowledgements	53
	Appendices	54
A	Wick rotation of correlators	55
A.1	Analytic continuation	55
A.2	Euclidean correlators are time ordered	55
A.3	Lorentzian correlators	56
A.4	An example	56

Chapter 1

Introduction

The conformal bootstrap offers a powerful constraining power to conformal field theories. It is what makes studying conformal field theories special. Radial quantization and the operator product expansion lie at the heart of conformal field theories. These two principles lead to everything that is special about CFTs. Crossing symmetry is the first step towards a constraint present in conformal field theories and forms the basis of the conformal bootstrap. The power of the conformal bootstrap has been implemented by many researchers to physical models, most famously the 2 and 3 dimensional Ising models. The error estimation by using the bootstrap philosophy is much smaller than when we use Monte Carlo simulations. So the philosophy is not just a pretty one. Its applications to physical models has proven its utility beyond the paper and pen. It is important to note the beauty and elegance of the construct itself. The constraining equations are powerful enough to give rise to these beautiful theorems we see exclusively in conformal field theories.

The inversion formula holds a special place in the conformal bootstrap paradigm. The existence of such a theorem itself highlights the amount of physical content present within the mathematics of conformal field theories. The motivation behind the inversion formula stemmed from the existence of a similar formula for S-matrices in the Froissart Gribov formalism. To this end, [3], came up with an ingenious way of deriving the formula in Lorentzian theory. This formula epitomises analyticity in spin. We will show an example of what the inversion formula aims to achieve. This will set up the motivation to study the formula more concretely.

An Example

Consider the function $f(E)$ which holds the following Taylor series expansion for low energies:

$$f(E) = \sum_{J=0}^{\infty} f_J E^J \quad (1.0.1)$$

$f(E)$ is defined such that it is analytic at all points except for branch cuts at real $|E| > 1$ and $|f(E)/E|$ is bounded at infinity. Refer figure (1) for the locations of the branch points and the branch cuts.

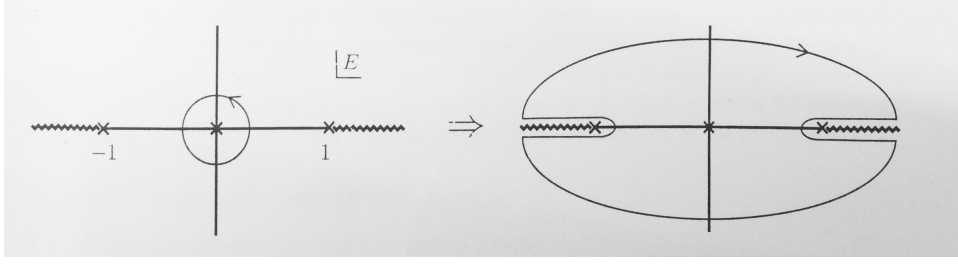


Figure 1.1: Branch points and branch cuts for $f(E)$ (Borrowed from [22])

Now the coefficient f_J can be isolated by the Cauchy integral formula. Thus we have:

$$\begin{aligned} f_J &= \frac{1}{2\pi i} \oint_{|E|<1} \frac{dE}{E} E^{-J} f(E) \\ &= \frac{1}{2\pi} \int_0^\infty \frac{dE}{E} E^{-J} (\text{Disc } f(E) + (-1)^J \text{Disc } f(-E)) \quad (J > 1) \end{aligned} \quad (1.0.2)$$

where

$$\text{Disc } f(E) = -i[f(E + i0) - f(E - i0)] \quad (1.0.3)$$

We have deformed the contour in the above integral in the manner highlighted by (1). Why has this been done? We have assumed that $|f(E)/E|$ is bounded which implies that the integrand behaves properly in that limit. Moreover, we have also added a constraint that $J > 1$. This is done so as to ensure that the arcs at infinity do not contribute, and essentially we have two contours hugging the branch cut in the manner of (4.3.3). This gives rise to the double discontinuity that appears in the above formula (1.0.2). Where do we get the $(-1)^J$ factor? There are two distinct regions where the integration is performed - the positive real axis and the negative real axis. For the integration over the negative real axis, we need to perform a change of variable in order to get an integrand similar to the one on the positive real axis. This change of variable results in the appearance of the extra $(-1)^J$ factor.

We frame the question in a different manner: if we have information about $f(E)$, can we determine the coefficients f_J ? The answer is yes and is given by the formula above. The above formula is analytic in J and thus it can be analytically continued to $J > 1$. But we need to remember that the key to the whole process was the behaviour of the integrand in the Regge limit (infinity arcs). We needed this to get the double discontinuity and get the analytic formula in (1.0.2) - analytic only for spins $J > 1$.

Why did we explain this example? Because, a similar method exists for the S-matrix Froissart Gribov method, except that there we use a Legendre polynomial expansion instead of a Taylor series expansion. This paved the way to look for analogous formula in conformal field theory. This is precisely the Inversion formula. For the inversion formula, $f(E)$ is replaced by the four points correlator and f_J represents the OPE coefficients. These coefficients will depend on whether we expand the four point function in the s, t or u channel. These coefficients hold information about the conformal field theory in question. To this end, if we know all CFT parameters, essentially we know everything there is

to know about the conformal field theory. before moving on we highlight some precursor conditions in which the formula holds:

- The external operators should be scalar and not spinning
- The final formula will be analytic only for $J > 1$ and not for all values of spin

We will highlight the importance of these two points in the report but it is important to always keep these at the back of our minds lest we forget to mention their significance.

A peep ahead

In chapter 2, we review some important preliminary concepts of the conformal bootstrap philosophy. These are standard tools of conformal field theory that we will require as the report progresses. We start by defining what conformal field theories are and how they differ from quantum field theories. We define the generators of conformal transformations and talk about conformal representations - the importance of the dilatation and the special conformal transformation generators. We then continue towards describing how operators and states are defined in conformal field theories. This is followed by talking about correlators in CFTs. The operator product expansion and the conformal blocks come next. The two main textbooks used for this section are [2] and [7]. Reviews on the bootstrap philosophy: [21, 17, 18] and chapter 2 of [16] offer a pretty comprehensive take on the subject matter with sufficient nuance. Following these preliminary discussions we move towards describing the shadow formalism and the principal series representation in CFTs. Most of the subject matter has been borrowed from [20]. Many of the derivations of the results we have stated in these sections can be found in [6] and [5].

In chapter 3, we talk about the spacetime derivation of the Lorentzian Inversion formula. this was presented in [22] as an alternative derivation of the inversion formula. We start by first getting the Euclidean inversion formula and then analysing techniques to analytically continue the formula to Lorentzian spacetime. First, we discuss how to get the formula for two dimensions. This is important because two dimensions will give us a brief peep into what we can expect in higher dimensions. Comments have been made as to why the two dimensional approach is somewhat less circuitous than its higher dimensional analogue. There are two different systems of cross ratios that are used in this and the following chapter. We have not gone into the nuances of these systems but [9] offers a very insightful review of these radial coordinates. We end this chapter by performing the analytical continuation in the cross ratio space as opposed to the Minkowski space and we show that the result is equivalent.

In chapter 4, we discuss the derivation of the inversion formula as presented by Caron-Huot in [3]. We start with a result which was presented in [4] and start our analysis from this juncture. In this section we highlight how exactly the CFT parameters connect themselves to the inversion formula. Here we introduce yet another coordinate system, highlight its importance and analyse analytic continuation in these coordinates too. We offer a heuristic argument as to why the entire process works and how we arrive at the final formula. The original arguments in [3] are also reviewed. We end the chapter by discussing the similarities and differences between the two trajectories of derivation.

In appendix [A](#), we detail the process of analytically continuing correlators from Euclidean space to Minkowski space. There are a number of nuances that need to be kept in mind while performing an analytic continuation. These are highlighted through an example in this appendix. [\[8\]](#) offers a brilliant review on these techniques and our material in this section is inspired from this paper.

We finally conclude our report by discussing the future prospects that this formula could point towards. This formula bases itself heavily on the result given in [\[14\]](#) and we highlight its importance in the text. We also talk about the present implications of these two results when we finally conclude our report. This report hopes to cover the physical aspects of the inversion formula as properly as it can. The report hopes to be a stepping stone to understanding the applications of the inversion formula in the near future.

Chapter 2

Conformal Field Theories

Conformal field theories form a group of field theories which are invariant under conformal transformations. These transformations form a bigger class of transformations than the familiar Lorentz transformations which form the symmetry group for quantum field theories. In this chapter, we will aim to review a few basic tenets of conformal transformations, some of their important properties and a few non-standard concepts which will serve us good in the following sections where we will use these results to derive the Inversion formula.

2.1 Definition

A conformal transformation is a coordinate transformation that preserves the form of the metric tensor upto a scale factor:

$$\delta_{\mu\nu} \frac{d\tilde{x}^\mu}{dx^\alpha} \frac{d\tilde{x}^\nu}{dx^\beta} = \Omega^2(x) \delta_{\alpha\beta} \quad (2.1.1)$$

If we perform a differential analysis on this equation (2.1.1) by taking the following transformation:

$$\tilde{x}^\mu = x^\mu + \epsilon^\mu \quad (2.1.2)$$

and feeding it into (2.1.1), we get the conformal killing equation:

$$\partial_\mu \epsilon_\nu + \partial_\nu \epsilon_\mu = c(x) \delta_{\mu\nu} \quad (2.1.3)$$

We will be working in Euclidean space in this entire chapter. Satisfying the killing equation are the following generators of symmetry:

$p_\mu = \partial_\mu$	translations	
$m_{\mu\nu} = x_\nu \partial_\mu - x_\mu \partial_\nu$	rotations	
$d = x^\mu \partial_\mu$	dilatations	(2.1.4)
$k_\mu = 2x_\mu(x \cdot \partial) - x^2 \partial_\mu$	special conformal transformations	

The corresponding conserved charges corresponding to these generators are given as:

$$Q_\epsilon = - \int dS_\mu \epsilon_\nu(x) T^{\mu\nu}(x) \quad (2.1.5)$$

where Q_ϵ is the conserved charge and $T^{\mu\nu}$ is the conserved current corresponding to the vector field $\epsilon = \epsilon^\mu(x)\partial_\mu$.

Inversions also form a symmetry of conformal transformations, however a conjugation of two special conformal transformations with a translation give an inversion, so its not considered as an additional symmetry. The exact relation is given as:

$$k_\mu = -Ip_\mu I \quad (2.1.6)$$

where

$$I : x^\mu \rightarrow \frac{x^\mu}{x^2} \quad (2.1.7)$$

These generators of symmetry form the $SO(d+1,1)$ symmetry group. So, we can rewrite the generators of conformal transformations as generators of transformations of $SO(d+1,1)$ transformations:

$$\begin{aligned} L_{\mu\nu} &= m_{\mu\nu} \\ L_{-1,0} &= d \\ L_{0\mu} &= \frac{1}{2}(p_\mu + k_\mu) \\ L_{-1,\mu} &= \frac{1}{2}(p_\mu - k_\mu) \end{aligned} \quad (2.1.8)$$

where

$$L_{ab} = -L_{ba} \quad (2.1.9)$$

$a, b \in -1, 0, 1, \dots, d$ and L_{ab} are the generators of the $SO(d+1,1)$ group. We define the Casimir operator as follows:

$$C = -\frac{1}{2}L_{ab}L^{ab} \quad (2.1.10)$$

this operator and its eigenvalue on some particular eigenfunctions will be important later.

2.2 Operators and Correlators

In this section, we define what we mean by operators in conformal field theories. The definition we use is similar to the way we define operators in quantum field theories. [21]. We then go on to define correlators of these operators. Depending on how the operators behave, the form of the correlators will be constrained by conformal symmetry. We don't give an explanation of how we arrive at the correlators we have presented. But, one can refer to [21] for further elucidation.

2.2.1 Operators

We define an operator like we do in quantum field theories. The commutator of a charge with an operator needs to be found out. The charge corresponds to the conserved currents of the generators of conformal transformations. We first define the action of a operator at the origin and then use the general

commutation relations between the generators to define their action at some general spacetime point. Thus, we define an operator as follows:

$$\begin{aligned} [M_{\mu\nu}, O^a(0)] &= (S_{\mu\nu})^a_b O^b \\ [D, O(0)] &= \Delta O(0) \end{aligned} \quad (2.2.1)$$

where $M_{\mu\nu}$ and D are the conserved charges corresponding to rotations and dilatations, respectively (from (2.1.5)). $S_{\mu\nu}$ are $SO(d)$ spin matrices and a & b are the spin indices. Δ is defined as the scaling dimension of the operator.

Use the commutation relations between the conserved charges, we get the following relations [21]:

$$[Q_\epsilon, O(x)] = \left(\epsilon \cdot \partial + \frac{\Delta}{d} (\partial \cdot \epsilon) - \frac{1}{2} (\partial_\mu \epsilon^\nu) S_{\mu\nu} \right) \quad (2.2.2)$$

2.2.2 Correlators

With these definitions, we can now proceed to define correlators of these operators. We will just mention the general form of these function. Again, a dedicated proof can be given for the following steps, but we will not require that amount of rigour in our main exercise. The notation followed will be: Δ_i is the scaling dimension of the operator insertion at x_i $O_i(x_i)$.

- Two point correlator for scalar operators:

$$\langle O_1(x_1) O_2(x_2) \rangle = \frac{\delta_{\Delta_1 \Delta_2}}{|x_1 - x_2|^{\Delta_1 + \Delta_2}} \quad (2.2.3)$$

- Three point correlator (scalar operators):

$$\langle O_1 O_2 O_3 \rangle = \frac{f_{123}}{x_{12}^{\Delta_1 + \Delta_2 - \Delta_3} x_{23}^{\Delta_2 + \Delta_3 - \Delta_1} x_{13}^{\Delta_3 + \Delta_1 - \Delta_2}} \quad (2.2.4)$$

Here we note the factor f_{123} . This is the one of the factors that we are interested in deriving from the inversion formula.

- Four point scalar operator correlator:

$$\langle O_1 O_2 O_3 O_4 \rangle = \frac{1}{(x_{12}^2)^{\frac{\Delta_1 + \Delta_2}{2}} (x_{34}^2)^{\frac{\Delta_3 + \Delta_4}{2}}} \left(\frac{x_{14}^2}{x_{24}^2} \right)^{\frac{\Delta_1 - \Delta_2}{2}} \left(\frac{x_{14}^2}{x_{13}^2} \right)^{\frac{\Delta_3 - \Delta_4}{2}} g(u, v) \quad (2.2.5)$$

where u and v are the cross ratios given by:

$$u = \frac{x_{12}^2 x_{34}^2}{x_{13}^2 x_{24}^2} \quad v = \frac{x_{23}^2 x_{14}^2}{x_{13}^2 x_{24}^2} \quad (2.2.6)$$

The reason behind this peculiar fact is that we can use conformal transformations to fix four points in a plane. Why can we choose this gauge? We follow the following steps:

- First use special conformal transformations so that $x_4 = \infty$.
- Then use translations to bring x_1 to 0.

- Then use rotations and dilatation to bring x_3 to 1.
- Use rotations so that x_2 lies in the 2D plane (x, y) .

Thus, we need just two independent variables. We can rewrite these cross ratios in the following form, in terms of χ and $\bar{\chi}$. The usage of this will be clear in the coming chapters.

$$u = \chi\bar{\chi} \quad v = (1 - \chi)(1 - \bar{\chi}) \quad (2.2.7)$$

These variables are quite independent and not necessarily complex conjugates of each other. If we work in the particular gauge as given by (2.2.2), then we have $\chi = x + iy$ and $\bar{\chi} = x - iy$ to be complex conjugates of each other. But, a priori, there is no reason to believe that these are related by a complex conjugation.

- Two spin-1 operators with dimension Δ : two point correlator:

$$\begin{aligned} \langle J^\mu(x) J_\nu(y) \rangle &= C_J \frac{I_\nu^\mu(x - y)}{(x - y)^{2\Delta}} \\ I_\nu^\mu &= \delta_\nu^\mu - 2 \frac{x^\mu x_\nu}{x^2} \end{aligned} \quad (2.2.8)$$

Again C_J is a CFT data similar to f_{ijk} referred to earlier.

- Three point function: one spin- l operator and two scalar operators:

$$\langle O_1(x_1) O_2(x_2) J^{\mu_1 \mu_2 \dots \mu_l}(x_3) \rangle = \frac{f_{O_1 O_2 J}(Z^{\mu_1 \dots \mu_l} - \text{traces})}{x_{12}^{\Delta_1 + \Delta_2 - \Delta_3 + l} x_{23}^{\Delta_2 + \Delta_3 - \Delta_1 - l} x_{31}^{\Delta_1 + \Delta_3 - \Delta_2 - l}} \quad (2.2.9)$$

where

$$Z^\mu = \frac{x_{13}^\mu}{x_{13}^2} - \frac{x_{23}^\mu}{x_{23}^2} \quad (2.2.10)$$

2.3 The Operator Product Expansion (OPE)

We first define what we mean by primary and descendants in conformal field theories. These are key to the basis of the operator product expansion. Then we move on to describe the operator product expansion. Operator product expansions can be done in quantum field theories too, however only for a region close to the origin. The expansion in conformal field theories is a bit more general.

2.3.1 Primaries and descendants

We saw in (2.2.1), the way to define operators in conformal field theories as specific representations of the conformal group. We define a primary operator as :

$$\begin{aligned} [d, O(0)] &= \Delta O(0) \\ [M_{\mu\nu}, O(0)] &= S_{\mu\nu} O(0) \\ [K_\mu, O(0)] &= 0 \end{aligned} \quad (2.3.1)$$

Now:

$$\begin{aligned} DK_\mu O(0) &= (\Delta - 1)K_\mu O(0) \\ DP_\mu O(0) &= (\Delta + 1)P_\mu O(0) \end{aligned} \quad (2.3.2)$$

P_μ acts like a raising operator and K_μ as a lowering operator. The operator with the lowest weight is the primary. Act on the primary with a D and we get higher weights. These are the descendants. Now, it can be proven that in any unitary CFT, a local operator can be written as a linear combination of primaries and descendants. Refer [21] for a detailed explanation for this fact.

2.3.2 Operator Product Expansion

The product of two operators in a conformal field theory can be expanded into a summation over primaries and descendants. That this was possible was mentioned in the earlier subsection. What precisely we will do here is that express the descendants as derivatives of primary operators, which will just give a summation over the primaries of the conformal field theory. This is the operator product expansion which is given by:

$$O_i^a(x_1)O_j^b(x_2) = \sum_k C_{ijk}^{ab}(x_{12}, \partial_2) O_k^c(x_2) \quad (2.3.3)$$

where a, b and c denote the spin indices for the operators belonging to different representations of the rotation group $SO(d)$. C_{ijk} is an operator which generates descendants of the primary operators it operates upon.

We can guess the mathematical nature of C_{ijk} . We can act on the left hand side and the right hand side of (2.3.3) with the conformal generators. This can give us the behaviour of C_{ijk} . If we perform an OPE expansion for two scalar operators then corresponding action of C_{ijk} on scalar primary operators is given by [21]:

$$C_{ijk}(x, \partial) \propto |x|^{\delta_k - \delta_i - \delta_j} (1 + \#x^\mu \partial_\mu + \#x^\mu x^\nu \partial_\nu \partial_\mu + \dots) \quad (2.3.4)$$

More generally, for spin operators in the expansion, the expansion is given by [20]:

$$\begin{aligned} O_i(x_1)O_j(x_2) &= f_{ijk} x_{12}^{\delta_k - \delta_i - \delta_j - l} x_{12\mu_1} \dots x_{12\mu_l} O^{\mu_1 \dots \mu_l}(x_2) \\ &\quad + \text{descendants} + \text{other multiplets.} \end{aligned} \quad (2.3.5)$$

We now use the OPE to deduce some things about 4 point functions and conformal blocks [21]. For a correlator of four operators, we can either perform an OPE expansion as [12][34] (s-channel), or [13][24] (t-channel) or [14][23] (u-channel). Now since the expansions have to be the same, these give constraining equations. These are the crossing symmetry equations.

If we expand (any channel would do) we get the following expression:

$$\langle O_1(x_1)O_2(x_2)O_3(x_3)O_4(x_4) \rangle = \sum_{\Delta, J} p_{\Delta, J} G_{\Delta, J}^{\Delta_i}(x_i) \quad (2.3.6)$$

where $G_{\Delta, J}^{\Delta_i}(x_i)$ is the conformal block. We sketch a proof for four scalar iden-

tical operators:

$$\begin{aligned}
\langle O(x_1)O(x_2)O(x_3)O(x_4) \rangle &= \sum_{\phi} f_{OO\phi}^2 C_a(x_{12}, \partial_2) C_b(x_{34}, \partial_4) \frac{I^{ab}(x_{24})}{x_{24}^{2\Delta_{\phi}}} \\
&= \frac{1}{x_{12}^{2\Delta_O} x_{34}^{2\Delta_O}} \sum_{\phi} f_{OO\phi}^2 g_{\Delta_{\phi}, J_{\phi}}(x_i)
\end{aligned} \tag{2.3.7}$$

We had calculated the four point function in (2.2.5). Equating the above equation (2.3.7) with (2.2.5), we get:

$$g(u, v) = \sum_{\phi} f_{OO\phi}^2 g_{\Delta_{\phi}, J_{\phi}}(x_i) \tag{2.3.8}$$

The connection between the expansions in (2.3.6) and in (2.3.7) is given by:

$$G_{\Delta_{\phi}, J_{\phi}}^{\Delta_O}(x_i) = \frac{1}{x_{12}^{2\Delta_O} x_{34}^{2\Delta_O}} g_{\Delta_{\phi}, J_{\phi}}(x_i) \tag{2.3.9}$$

The conformal block is entirely fixed by conformal symmetry. The information about the CFT data is present in $p_{\Delta, J}$. Once we have defined the conformal block and expressed the four point function as a series in conformal blocks summed over the space of operators appearing in the OPE of the four operators involved, we now mention some interesting properties of the conformal block [20]:

- Its conformally invariant.
- Its an eigen-function of the 1+2 conformal Casimir (2.1.10) with an eigenvalue equal to $d(d - \Delta) + l(l + d - 2)$.
- The small x_{12} limit of the conformal block given by:

$$g_O(u, v) \propto x_{12}^{\Delta-l} x_{12\mu_1} \dots x_{12\mu_l} \langle O^{\mu_1 \dots \mu_l}(x_2) \phi_3(x_3) \phi_4(x_4) \rangle \tag{2.3.10}$$

Refer [6] for a rigorous discussion of these properties. We will use these properties to define an integral in the next section which will share the same properties listed above. This integral will be an interesting beast to study and will prove to be the basis on which the first derivation of the Lorentzian inversion formula will rest upon.

2.4 Shadow formalism

If we consider an operator $O(x)$ in a d -dimensional CFT with scaling dimension Δ , we can define a non-local shadow operator corresponding to it $\tilde{O}(x)$ with a scaling dimension equal to $d - \Delta$.

$$\tilde{O}(y_1) = \int d^d y_2 \frac{O(y_1)}{|y_1 - y_2|^{2(d-\Delta)}} \tag{2.4.1}$$

Now consider the following integral:

$$I = \int d^d x O(x) |0\rangle\langle 0| \tilde{O}(x) \quad (2.4.2)$$

It can be easily shown that the above integral is conformally invariant. Now consider the integral:

$$J = \Psi_{\Delta,J}^{\Delta_i}(x_i) = \int d^d x_5 \langle O_1(x_1) O_2(x_2) O(x_5) \rangle \langle \tilde{O}(x_5) O_3(x_3) O_4(x_4) \rangle \quad (2.4.3)$$

Since I is invariant, so is J invariant under conformal transformations. An interesting note about the integral J is that it also satisfies the three properties of the conformal block highlighted in the earlier section. Now, we will show an important consequence of this fact.

For our analysis in the upcoming sections, we will rename the integral J by $\Psi_{\Delta,J}^{\Delta_i}$ where Δ_i s are the scaling dimensions of the operators O_i and Δ is the scaling dimension of O . \tilde{O} is the shadow operator corresponding to O . This integral is known as the conformal partial wave. We can express this integral as a sum over a conformal block and the corresponding shadow block. The exact derivation of the following result is given in [22] and [6]:

$$\Psi_{\Delta,J}^{\Delta_i}(x_i) = K_{\Delta,J}^{\Delta_3,\Delta_4} G_{\Delta,J}^{\Delta_i}(x_i) + K_{\Delta,J}^{\Delta_1,\Delta_2} G_{\tilde{\Delta},J}^{\Delta_i}(x_i) \quad (2.4.4)$$

where $K_{\Delta,J}^{\Delta_3,\Delta_4}$ and $K_{\Delta,J}^{\Delta_1,\Delta_2}$ are constants accompanying the respective conformal blocks, the definition for which has been given in (2.3.6). This constant is defined as:

$$K_{\Delta,J}^{\Delta_1,\Delta_2} = \left(-\frac{1}{2}\right)^J \frac{\pi^{\frac{d}{2}} \Gamma(\Delta - \frac{d}{2}) \Gamma(\Delta + J - 1) \Gamma(\frac{\tilde{\Delta} + \Delta_1 - \Delta_2 + J}{2}) \Gamma(\frac{\tilde{\Delta} + \Delta_2 - \Delta_1 + J}{2})}{\Gamma(\Delta - 1) \Gamma(d - \Delta + J) \Gamma(\frac{\Delta + \Delta_1 - \Delta_2 + J}{2}) \Gamma(\frac{\Delta + \Delta_2 - \Delta_1 + J}{2})} \quad (2.4.5)$$

This is an important fact. The conformal partial wave has the same properties as the conformal block and as can be seen from the above equation, it can be expressed as a sum over two conformal blocks - one standard block and one shadow block.

2.5 Principal Series representation

Why are we so interested in the integral (2.4.3)? The conformal partial waves when expressed in the principal series representation form a square integrable complete set of functions. In the principle series representation, the dimensions are unphysical and complex in the form $\Delta = \frac{d}{2} + ir$ where r is some non-negative real number. This is an advantage because then when we look at equation (2.4.4), then we can see that the dimension parameter in the subscript of the shadow block will just be a complex conjugate of the dimension of the conformal block¹. Another advantage of the principle series representation is that these partial waves with complex dimensions also form an orthogonal basis. This orthogonal inner product is conformally invariant which will turn out to

¹ $(\frac{d}{2} + ir)^* = \frac{d}{2} - ir = d - (\frac{d}{2} + ir)$

be convenient as we will see in the future analysis. The inner product is given as:

$$\begin{aligned} \left(\Psi_{\Delta,J}^{\Delta_i}(x_i), \Psi_{\tilde{\Delta},J}^{\tilde{\Delta}_i}(x_i) \right) &= \int \frac{d^d x_1 \dots d^d x_4}{\text{Vol}(\text{SO}(d+1,1))} \Psi_{\Delta,J}^{\Delta_i}(x_i) \Psi_{\tilde{\Delta},J}^{\tilde{\Delta}_i}(x_i) \\ &= n_{\Delta,J} 2\pi \delta(r - r') \delta_{J,J'} \end{aligned} \quad (2.5.1)$$

where

$$n_{\Delta,J} = \frac{K_{\tilde{\Delta},J}^{\Delta_3,\Delta_4} K_{\Delta,J}^{\tilde{\Delta}_3,\tilde{\Delta}_4} \text{vol}(S^{d-2})}{\text{vol}(\text{SO}(d-1))} \frac{(2J+d-2)\pi\Gamma(J+1)\Gamma(J+d-2)}{2^{d-2}\Gamma(J+\frac{d}{2})^2} \quad (2.5.2)$$

The 4 points $x_1 \dots x_4$ are invariant under simultaneous conformal transformations and hence in order to keep the integral finite, we divide the integral by the volume of the conformal group in d dimensions (in Euclidean spacetime). This is precisely the group $\text{SO}(d+1,1)$. The exact proof of the orthonormality and completeness of these functions can be found in [22]. The value of $n_{\Delta,J}$ has also been calculated.

The principal series representation will play an important role in the derivation of the Lorentzian inversion formula, as we will see in the upcoming section. To this end, each of the properties that we have highlighted in this section will play a crucial role.

Chapter 3

Spacetime derivation

The first method of deriving the inversion formula was given in the recent paper [22]. This was an alternate way of deriving the inversion formula. In this chapter, we will go through this derivation. We will solve explicitly the two dimensional case, since we can clearly see the essence of the derivation taking shape. Then we move on to describe the derivation for higher dimensions. We highlight some complications that arise in the dimensional case. We end the chapter by comparing the method with Simon Caron-Huot's approach which has been detailed in the next chapter.

3.1 Introduction

We will start with the principal series representation. As mentioned in the earlier section, the principal series form an orthonormal basis of the eigenspace corresponding to the $\Delta(d-\Delta)+J(J+d-2)$ eigenvalue of the conformal Casimir (2.1.10).

Now, consider the four point correlator. Since the principle series representation forms a complete basis, a 4-point function (the normalisable part, to say the least) can be expanded into these orthonormal functions. This is a process that is entirely analogous to the Fourier expansion of a translation invariant function. Therefore we write the following expression:

$$\langle O_1(x_1)O_2(x_2)O_3(x_3)O_4(x_4) \rangle = \sum_{J=0}^{\infty} \int_{\frac{d}{2}}^{\frac{d}{2}+i\infty} \frac{d\Delta}{2\pi i} \frac{I_{\Delta,J}}{n_{\Delta,J}} \Psi_{\Delta,J}^{\Delta_i}(x_i) + (\text{non - norm.}) \quad (3.1.1)$$

where $I_{\Delta,J}$ are the coefficients of accompanying the partial waves in the expansion. A 4-point function might not be square integrable. As such, care needs to be taken when expressing them as sums of principal series functions which are square integrable. There are two major source of these non-normalizable contributions: (1) identity operator, (2) scalar operators with $\Delta \leq d/2$. We will not go into much detail as to why these contributions are non-normalisable, as they do not affect directly the analysis that we will be carrying out.

We postulate the CFT data is encoded in the coefficients $I_{\Delta,J}$ in the expansion (3.1.1). A detailed explanation of this statement is made in the subsection (4.2).

For now, we will assume that the the supposed CFT data alluded to is somehow encoded in $I_{\Delta,J}$. This CFT data is precisely the coefficient accompanying the respective operator in the OPE expansion. Therefore, what we will be doing is inverting (3.1.1) using (2.5.1) in order to isolate out $I_{\Delta,J}$, in which we are interested in. Again, analogies can be drawn to Fourier analysis. In order to isolate the Fourier expansion coefficients, we perform an inverse Fourier transform. Following up with this spirit in mind, we get:

$$\begin{aligned} I_{\Delta,J} &= \left(\langle O_1 \dots O_4 \rangle, \Psi_{\Delta,J}^{\tilde{\Delta}_i} \right) \\ &= \int \frac{d^d x_1 \dots d^d x_4}{\text{Vol}(\text{SO}(d+1,1))} \langle O_1 \dots O_4 \rangle \Psi_{\Delta,J}^{\tilde{\Delta}_i} \end{aligned} \quad (3.1.2)$$

(3.1.2) is precisely the equation that we wish to solve. The analysis ends with performing this integral till we end up with an integral over cross ratios. Also, we wish to solve the theory in Lorentzian spacetime. Till now, we were working in Euclidean spacetime, so we will need to perform a Wick rotation in an intermediate step. We will run into problems as Wick's rotation is also not that trivial since there are many singularities and branch points that we need to consider. We will detail these steps first for the 2 dimensional case as it is significantly much simpler for this case, then generalise the analysis to higher dimensions with enough motivation as to what is so different between two and higher dimensions.

3.2 2 dimensions

Before performing a general derivation for d dimensions, in this section, we will solve for the simpler two dimensional case. This will give us a feel of the derivation - what its salient features are and the nuances we need to keep in mind.

3.2.1 Euclidean Inversion formula

Consider a two dimensional conformal field theory. We will get the CFT data by deriving the inversion formula for the simplest case where the external dimensions of the operators are all equal ¹, i.e $\Delta_1 = \Delta_2 = \Delta_3 = \Delta_4 = \Delta_O$. Since, we are talking about two dimensions, the conformal group in Euclidean spacetime is $SO(3,1)$ which is isomorphic to $SL(2, \mathbb{R}) \times SL(2, \mathbb{R})$. Conformal field theories in two dimensions are a bit different from their higher dimensional analogues. To this end, defining an operator in 2D CFTs requires two parameters. These factors or parameters are given by : h and \bar{h} . The scaling dimension in two dimensions varies as $\Delta = h + \bar{h}$ and the spin is given by $J = |h - \bar{h}|$. Therefore when we resort to eq (2.4.3), we get the following partial wave definition:

$$\Psi_{h,\bar{h}}^{\Delta_O}(z_i, \bar{z}_i) = \frac{1}{|z_{12}|^{2\Delta_O} |z_{34}|^{2\Delta_O}} \Psi_{h,\bar{h}}(z_i, \bar{z}_i) \quad (3.2.1)$$

¹External operators correspond to the 4 functions whose correlation function is known. In eq (3.1.2), the correlator inside the integral is a function of these 4 external operators. $I_{\Delta,J}$ corresponds to the coefficient of the operator O in (2.3.3) in the OPE expansion of two external operators (in this case taken to be the same).

where

$$\Psi_{h,\bar{h}}(z_i, \bar{z}_i) = \int d^2 z_5 \left(\frac{z_{12}}{z_{15} z_{25}} \right)^h \left(\frac{\bar{z}_{12}}{\bar{z}_{15} \bar{z}_{25}} \right)^{\bar{h}} \left(\frac{z_{12}}{z_{15} z_{25}} \right)^{1-h} \left(\frac{\bar{z}_{12}}{\bar{z}_{15} \bar{z}_{25}} \right)^{1-\bar{h}} \quad (3.2.2)$$

The above expansion (3.2.1) is completely analogous to the representation of a four point function (2.3.9) and (2.2.5). Therefore, we can draw an interesting analogy by saying that since $g(u, v)$ is an eigen-function of the Casimir, $\Psi_{h,\bar{h}}$ is also an eigen-function of the two dimensional Casimir operator. In the earlier sections, we have shown how the (2.4.3) is a sum of two conformal blocks - a normal block and the corresponding shadow block. The above analogy stems from this fact itself.

As highlighted briefly before, two dimensional CFTs are special. We will mention some more special properties that hold true specifically for 2 dimensional conformal field theories. We will not be rigorous in our approach, but the reader can refer to [2] or [7] for a thorough discussion of these ideas. Though these are not important for understanding the derivation, it gives an important perspective as to how 2 dimensional CFTs differ from their higher dimensional cousins. The operators, functions and the states in two dimensions can be considered as consisting of two distinct sectors - a holomorphic sector and an antiholomorphic sector. These sectors can be dealt with separately and hence the notion of the two parameters h and \bar{h} . This fact implies that the symmetric traceless representation of 2D CFT group is reducible and we have considered only one part of the partial wave. The complete partial wave would have been $\Psi_{h,\bar{h}} + \Psi_{\bar{h},h}$. Hence, out of the two representations - (0,2) and the (2,0) possible, we will consider just one. This point will turn out to be important later. The two parts of the two different representation turn out to simplify matters significantly for the two dimensional case. The main crux of the argument lies in the fact that this simplification leads to an integral which is not infinite. We will return to this point when we come to the higher dimensional case.

Now that some comments have been made exclusive to the two dimensional case, we embark upon getting the inversion formula. The two dimensional analogue of (3.1.1) is given by:

$$\langle O_1(z_1) O_2(z_2) O_3(z_3) O_4(z_4) \rangle = \sum_{J=0}^{\infty} \int_0^{\infty} \frac{dr}{2\pi} \frac{I_{h,\bar{h}}}{n_{h,\bar{h}}} \Psi_{h,\bar{h}}^{\Delta_O}(z_i) + (\text{non-norm.}) \quad (3.2.3)$$

where

$$\begin{aligned} h &= \frac{1+l+ir}{2} \\ \bar{h} &= \frac{1-l+ir}{2} \end{aligned} \quad (3.2.4)$$

and the analog of the orthogonality relation (2.5.1) is given by:

$$\begin{aligned} \left(\Psi_{h,\bar{h}}^{\Delta_O}, \Psi_{1-h',1-\bar{h}'}^{\tilde{\Delta}_O} \right) &= n_{h,\bar{h}} 2\pi \delta(r-r') \delta_{l,l'} \\ n_{h,\bar{h}} &= -\frac{2\pi^3}{(2h-1)(2\bar{h}-1)} \end{aligned} \quad (3.2.5)$$

where the shadow dimension of an (h, \bar{h}) operator is $(1-h, 1-\bar{h})$ and $\tilde{\Delta}_O =$

$2 - \Delta_O$ We use (3.1.2) to get $I_{h,\bar{h}}$:

$$I_{h,\bar{h}} = \int \frac{d^2 z_1 \dots d^2 z_4}{\text{Vol}(\text{SO}(3,1))} \langle O_1(z_1) O_2(z_2) O_3(z_3) O_4(z_4) \rangle \Psi_{1-h,1-\bar{h}}^{\tilde{\Delta}_O}(z_i, \bar{z}_i) \quad (3.2.6)$$

The above integral is invariant under simultaneous conformal transformations. So we fix a convenient gauge to calculate the integral further. This is equivalent to picking up a particular orbit in the phase space of all possible equivalent configurations which would contribute to the integral equally. Chosen gauge: $z_1 = 0, z_2 = \chi, z_3 = 1, z_4 = \infty$. Using this gauge gives a Faddeev Popov determinant of 1 so that we get no change in the measure of the integral (3.2.6). To get an idea of how the calculation of the Faddeev Popov determinant is done, the reader can refer to [13] and [15]. Therefore, we get:

$$I_{h,\bar{h}} = \int \frac{d^2 \chi}{|\chi|^{4-2\Delta_O}} \langle O_1(0) O_2(\chi) O_3(1) O_4(\infty) \rangle \Psi_{1-h,1-\bar{h}}(0, \chi, 1, \infty) \quad (3.2.7)$$

In fact, if we check (2.2.6), we can clearly see that

$$u = \chi \bar{\chi} \quad v = (1 - \chi)(1 - \bar{\chi}) \quad (3.2.8)$$

We will use the terms u, v and $\chi, \bar{\chi}$ interchangeably as cross-ratios. What we have got in (3.2.7) is the Euclidean version of the inversion formula. We want the Lorentzian version. For this, we need to fix gauge in a different manner² and then perform a Wick rotation. Now, we expand the partial wave in the integral (3.2.6) using the expansion given in (3.2.1) and (3.2.2) and fix the gauge as follows: $z_1 = 1, z_2 = 0, z_5 = \infty$. The choice that z_5 is taken to be at infinity is important. In the higher dimensional case, it will become clearer that the region we would integrate over in Lorentzian spacetime will have z_5 spacelike separated from each of the other 4 points. So, we get the following integral over the coordinates z_3 and z_4 .

$$I_{h,\bar{h}} = \int \frac{d^2 z_3 d^2 z_4}{|z_{34}|^{4-2\Delta_O}} \langle O_1 O_2 O_3 O_4 \rangle z_{34}^h \bar{z}_{34}^{\bar{h}} \quad (3.2.9)$$

The above integral is an integral over complex variables. Also the functions involved are complex functions. Therefore, to maintain the finiteness and single-valuedness of the above integral, it is important to note that the spin J has to be an integer.

3.2.2 Wick rotation

Now we perform the Wick rotation. We had obtained the Euclidean version of the inversion formula in (3.2.7) and we now wish to find the Lorentzian inversion formula. There is a definite motivation as to why we need the formula in Minkowski space. The entire physical universe exists in Lorentzian spacetime. So it only makes sense for a physical theory, in this case a formula to determine the physical CFT parameters, to be described in Lorentzian signature. Another motivation is that the inversion formula is non-intuitive. Somehow, just

²Why this different gauge? We will get a definite motivation when we consider this point in the higher dimensional case.

using complex analysis, we are getting something physical. There must exist some physical facts that we are implementing behind the curtains to get to this formula. As we will see in this section, one physical reason is the causality constraint. In our final expression, we will end up integrating over two Lorentzian patches in which these 4 coordinates will have a fixed spacelike or timelike relationship with others. This is one physical feature we can naively see. But there might be more to the formula than meets the eye.

Before performing a Wick rotation, first we move to lightcone coordinates.

$$u = x - t \quad v = x + t \quad (3.2.10)$$

Normal Feynman continuation via Wick's rotation is given by:

$$\tau = (i + \epsilon)t \quad (3.2.11)$$

where τ is the Euclidean time and t is the Lorentzian time coordinate. For a detailed discussion of Wick rotation, refer to appendix (A). The distance formula now becomes:

$$|z|^2 = x^2 + \tau^2 = x^2 - t^2 + i\epsilon = uv + i\epsilon \quad (3.2.12)$$

. Therefore in the lightcone gauge, the measure in (3.2.9) becomes:

$$d^2z = d\tau dx = \frac{i}{2} du dv \quad (3.2.13)$$

and the integral becomes:

$$I_{h,\bar{h}} = -\frac{1}{4} \int \frac{du_3 du_4 dv_3 dv_4}{(u_{34} v_{34})^{2-\Delta_O}} < O_1 O_2 O_3 O_4 > u_{34}^h v_{34}^{\bar{h}} \quad (3.2.14)$$

This was just a analytical continuation to Lorentzian space. But this is not as straightforward as it seems. We can analyse this continuation in two complex planes: corresponding to u and v . We will encounter singularities as we Wick rotate the Euclidean integral to the Lorentzian space. These singularities correspond to the collision of the points leading to infinities arising from the correlator. This collision means that the points in question become light-like separated. Hence, singularities in the correlator arise when any two operators in the correlator become light-like separated. Therefore, as before if we fix the points $z_1 = 1$ and $z_2 = 0$ (i.e $u_1 = v_1 = 1$ and $u_2 = v_2 = 0$ from (3.2.10)), we have the following four equations corresponding to the branch points of the integrand in eq (3.2.14):

$$\begin{aligned} u_3 v_3 + i\epsilon &= 0 & (3 \rightarrow 2) \\ u_4 v_4 + i\epsilon &= 0 & (4 \rightarrow 2) \\ (1 - u_3)(1 - v_3) + i\epsilon &= 0 & (3 \rightarrow 1) \\ (1 - u_4)(1 - v_4) + i\epsilon &= 0 & (4 \rightarrow 1) \\ (u_3 - u_4)(v_3 - v_4) + i\epsilon &= 0 & (3 \rightarrow 4) \end{aligned} \quad (3.2.15)$$

The kinematics in the complex plane for u_3, v_3, u_4 and v_4 will be governed by these singularities (3.2.15). Refer to appendix (A) for a discussion of kinematics similar to these through an example. The appendix also shows how branch points and branch cuts affect analytic continuation. Here, we will just use the results and skim past the details.

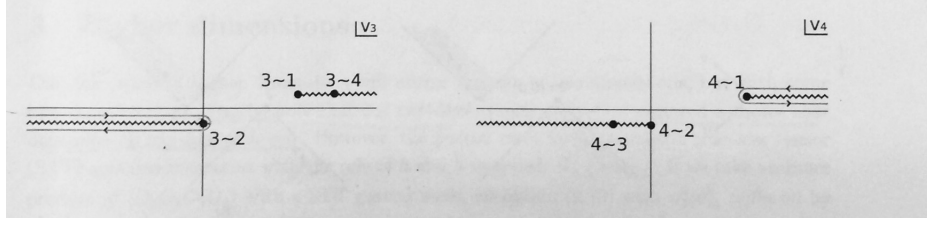


Figure 3.1: The sub-figure on the left gives the v_3 complex plane and the sub-figure on the right is the complex plane of v_4 .(Borrowed from [22])

The integral (3.2.14) involves four complex integration variables. We fix two variables u_3 and u_4 and interest ourselves with performing the integration over v_3 and v_4 , i.e we will first perform an integral over the v_i coordinates and then over the u_i coordinates. The integration range for these two variables v_3 and v_4 is 0 to ∞ . In order to keep the value of the integral finite, one needs to perform some sanity checks. Therefore, the following two assumptions are made:

- The behaviour of the four point function in the Regge limit is not abnormal and its value does not blow off to infinity. The Regge limit is defined precisely in the manner described above - v_3 and v_4 going to infinity. This is a very important point and holds the key to the entire physics of the problem. The fact that the four point functions of the theory do not behave in a strange manner at infinity is paramount to calculate the CFT data for the theory.
- The spin of the operators whose four point function we are using to calculate $I_{h, \bar{h}}$, is positive. Since we have fixed u_3 and u_4 , we deal with the term $v_{34}^{\bar{h}}$ in the integrand with $\bar{h} = \frac{\Delta - J}{2}$. It is clear to see why the spin has to be positive - the integral would blow up if it hadn't. If the spin would have been negative, we would have fixed v_3 and v_4 and integrated over u_3 and u_4 . We would have then dealt with the term u_{34}^h where $h = \frac{\Delta + J}{2}$, which would have forced us to assume the spin to be negative to maintain the finiteness of the integral.

Above, we have explained the nuances of the process, we can perform the integration. Since we are first performing the integral over the v_i coordinates and keep the u coordinates fixed, the above assumptions will constrain the values of u_i and v_i to specific Lorentzian patches for a non-vanishing integral.

The figure (3.2.2) shows the kinematics of Wick's rotation in the two complex planes v_3 and v_4 . The diagrams show the points where the branch points as highlighted in (3.2.15) occur. The appropriate branch cuts area also shown. As mentioned before when we mentioned the assumptions, the integration contour can be peeled away from infinity as the contributions die out in the Regge limit.

As can be inferred from (3.2.15), each of the two complex planes v_3 and v_4 consist of three collisions each and therefore, three branch points. The integral (3.2.14) is non-zero only if the contour around infinity is wound around the way it has been done in the diagram. A non-vanishing integral will occur only if one singularity is on the opposite side of the axis separated from the other two. This gives rise to two regions. This situation can be managed by fixing u_3, u_4

such that they satisfy the inequality $0 < u_3, u_4 < 1$.

If we analyse the sub-figure on the left in (3.2.2), where we have drawn the complex plane for the region $0 < u_3 < u_4 < 1$, we see that the contour moves around the branch point where 3 and 2 become light-like separated. As can be seen from appendix A, this leads to a flip in the order of operators appearing in the correlator. In this case, operators O_3 and O_2 will flip giving rise to the appearance of the commutator $[O_3, O_2]$ in the correlator. From the sub-figure on the right in (3.2.2), we see the appearance of the commutator $[O_1, O_4]$. Therefore an integral in this region gives rise to the double commutator $[O_3, O_2][O_1, O_4]$. On the other hand, an integral over the region $0 < u_4 < u_3 < 1$ gives rise to the double commutator $[O_4, O_2][O_1, O_3]$. Thus we can finally write the final integral from (3.2.14) as an integral over two Lorentzian patches:

$$I_{h,\bar{h}} = -\frac{(-1)^J}{4} \int_{R_1} \frac{du_3 dv_4 du_4 dv_4}{(u_{34} v_{34})^{2-\Delta_O}} < [O_3, O_2][O_1, O_4] > u_{43}^h v_{43}^{\bar{h}} \\ - \frac{1}{4} \int_{R_2} \frac{du_3 dv_4 du_4 dv_4}{(u_{34} v_{34})^{2-\Delta_O}} < [O_4, O_2][O_1, O_3] > u_{34}^h v_{34}^{\bar{h}} \quad (3.2.16)$$

where the integration regions are given by:

$$\begin{aligned} R_1 &\rightarrow v_3 < 0, & v_4 > 1, & 0 < u_3 < u_4 < 1 \\ R_1 &\rightarrow 4 > 1; 2 > 3; (4,1) \text{ and } (2,3) \text{ timelike separated} \\ R_2 &\rightarrow v_3 > 1, & v_4 < 0, & 0 < u_4 < u_3 < 1 \\ R_2 &\rightarrow 3 > 1; 2 > 4; (3,1) \text{ and } (2,4) \text{ timelike separated} \end{aligned} \quad (3.2.17)$$

Notice the difference between the two integrands being integrated above in (3.2.16). The first integral is accompanied by an extra $(-1)^J$. This is due to the fact, we get an extra $(-1)^J$ factor when moving from the Euclidean version to the Lorentzian version i.e $z_{34}^h \bar{z}_{34}^{\bar{h}}$ changes to $(-1)^J u_{43}^h v_{43}^{\bar{h}}$. This is quite similar to the equation we analysed in the introduction (1.0.2).

The above formula (3.2.16) is the Lorentzian inversion formula, where we integrate the correlator along with some measure factors over two Lorentzian regions. These Lorentzian regions also contain information about the causal relationship between the 4 points involved in the correlator. For the first Lorentzian patch R_1 pairs of points $(4>1)$ and $(2>3)$ are time-like separated. The other points are all space-like separated from each other. On the other hand, for the second Lorentzian patch R_2 , $(3>1)$ and $(2>4)$ are timelike separated and other pairs are space-like separated. Similar causal relationship between the four points will also hold in the higher dimensional case.

Also, it is important to note that, as we highlighted earlier, that we completed the analysis above having used the assumption that the spin was an integer. In (3.2.16), we have arrived at a formula which is analytic. We can analytically continue the formula to all values of spin. Single valuedness will also not be affected which was the primary problem we encountered in (3.2.9), since the inversion formula is now an integral over real valued variables. This is a very surprising, that starting with an assumption to maintain singlevaluedness, we have arrived at a single-valued formula that can be analytically continued to all values of spin. Keeping in mind the assumptions we made earlier, analytical continuation can be done only over the region $J \geq 0$. In order to maintain the finiteness of the integrand in the Regge limit, this restriction on the spin has

to be made. The appendix D.2 of [22] offers a more nuanced approach to the Wick rotation we have performed above. This gives a more stringent condition on the spin ,i.e $J > 1$.

We now convert the integral (3.2.16) into an integral over cross ratios. This is possible because of the new gauge we chose ($z_1 = 1, z_2 = 0$ and $z_5 = \infty$). More light on this point will be shed when we consider the higher dimensional case.

3.2.3 The final formula

Since we have fixed the gauge and hence the coordinates for 2 points: $u_1 = v_1 = 1$ and $u_2 = v_2 = 0$, we get the following expressions for the cross ratios:

$$\begin{aligned}\chi &= \frac{u_{34}}{(u_3 - 1)u_4} \\ \bar{\chi} &= \frac{v_{34}}{(v_3 - 1)v_4}\end{aligned}\tag{3.2.18}$$

Since we want to express (3.2.16), as an integral over the cross ratios over two Lorentzian patches, we will use (3.2.18) to rewrite (3.2.16). This is possible since (3.2.18) can be used to solve for u_3 and v_3 and then the integral over u_4 and v_4 can be performed. The integrand that is left will be just 4-point correlators multiplying the $SL(2, \mathbb{R})$ conformal blocks.

$$\begin{aligned}k_{2h}(\chi) &= \chi^h {}_2F_1(h, h, 2h, \chi) \\ \hat{k}_{2h}(\bar{\chi}) &= \chi^h {}_2F_1(h, h, 2h, \bar{\chi})\end{aligned}\tag{3.2.19}$$

where ${}_2F_1$ is the hypergeometric function. Conformal blocks in two dimensions are hypergeometric equations. Refer [5] for a proof of this statement. The entire simplified expression is given below:

$$\begin{aligned}I_{h, \bar{h}} &= -\frac{1}{4} \frac{\Gamma(h)^2 \Gamma(1 - \bar{h})^2}{\Gamma(2h) \Gamma(2 - 2\bar{h})} \left[(-1)^J \int_0^1 \int_0^1 \frac{d\chi d\bar{\chi}}{(\chi\bar{\chi})^{2-\Delta_O}} < [O_3, O_2][O_1, O_4] > k_{2h}(\chi) k_{2-2\bar{h}}(\bar{\chi}) \right. \\ &\quad \left. + \int_{-\infty}^0 \int_{-\infty}^0 \frac{d\chi d\bar{\chi}}{(\chi\bar{\chi})^{2-\Delta_O}} < [O_4, O_2][O_1, O_3] > \hat{k}_{2h}(\chi) \hat{k}_{2-2\bar{h}}(\bar{\chi}) \right]\end{aligned}\tag{3.2.20}$$

Once we derive the inversion formula by the method given in [3], a connection can be made to the paper's notation of $c(J, \Delta)$ by the following relation:

$$c(J, \Delta) = \frac{(-1)^J}{2\pi^2} \frac{\Gamma(h)^2}{\Gamma(2h - 1)} \frac{\Gamma(2 - 2\bar{h})}{\Gamma(1 - \bar{h})^2} I_{h, \bar{h}}\tag{3.2.21}$$

Thus, (3.2.20) is the final Lorentzian inversion formula for the two dimensional case in its full glory, expressed as an integral in the cross-ratio space and over two Lorentzian patches. A similar approach will hold for the higher dimensional case as we will highlight next, albeit the fact that we will run into some difficulties not encountered in this simpler scenario.

3.3 Higher dimensions

The higher dimensional case will follow the same template of steps as were used in the 2 dimensional case. There are a few extra steps that need to be taken since the higher dimensional conformal field theories offer more to the table do 2D CFTs

3.3.1 Euclidean inversion formula

Again we will start with conformal partial wave as defined in (2.4.3). The external operators for this inversion formula are scalars. The running operators in the OPE can have spin. With this mind, in eq (2.4.3), O_1, O_2, O_3 and O_4 are scalar operators but O can be spinning. Therefore, using (2.2.9) and (2.2.10), we solve the three point functions in (2.4.3). Therefore, after doing these manipulations, we get:

$$\begin{aligned} \Psi_{\Delta,J}^{\Delta_i}(x_i) &= \int d^d x_5 \frac{1}{|x_{12}|^{\Delta_1+\Delta_2-\Delta} |x_{15}|^{\Delta_1+\Delta-\Delta_2} |x_{25}|^{\Delta_2+\Delta-\Delta_1}} \\ &\times \frac{1}{|x_{34}|^{\Delta_3+\Delta_4-\tilde{\Delta}} |x_{35}|^{\Delta_3+\tilde{\Delta}-\Delta_4} |x_{45}|^{\Delta_4+\tilde{\Delta}-\Delta_3}} \hat{C}_J(\eta) \end{aligned} \quad (3.3.1)$$

where η has been defined as:

$$\eta = \frac{|x_{15}||x_{25}|}{|x_{12}|} \frac{|x_{35}||x_{45}|}{|x_{34}|} \left(\frac{\vec{x}_{15}}{x_{15}^2} - \frac{\vec{x}_{25}}{x_{25}^2} \right) \cdot \left(\frac{\vec{x}_{35}}{x_{35}^2} - \frac{\vec{x}_{45}}{x_{45}^2} \right) \quad (3.3.2)$$

and the Gegenbauer polynomial \hat{C}_J appears in the integral in the following representation:

$$|n|^J |m|^J \hat{C}_J\left(\frac{n \cdot m}{|n||m|}\right) = (n^{\mu_1} \dots n^{\mu_J} - \text{traces})(m^{\mu_1} \dots m^{\mu_J} - \text{traces}) \quad (3.3.3)$$

Also,

$$\begin{aligned} \hat{C}_J(x) &= \frac{\Gamma(J+1)\Gamma(\frac{d-2}{2})}{2^J \Gamma(J+\frac{d-2}{2})} C_J^{d/2-1} \\ C_J^{d/2-1}(x) &= \frac{\Gamma(J+d-2)}{\Gamma(J+1)\Gamma(d-2)} F_1(-J, J+d-2, \frac{d-1}{2}, \frac{1-x}{2}) \end{aligned} \quad (3.3.4)$$

If we use the definition of (2.4.3) to expand eq (3.1.2), we can express $I_{\Delta,J}$ as:

$$I_{\Delta,J} = \int \frac{d^d x_1 d^d x_2 d^d x_3 d^d x_4}{\text{vol}(\text{SO}(d+1,1))} \langle O_1 O_2 O_3 O_4 \rangle \langle \tilde{O}_1 \tilde{O}_2 \tilde{O}^{\mu_1 \dots \mu_J} \rangle \langle O_{\mu_1 \dots \mu_J} \tilde{O}_3 \tilde{O}_4 \rangle \quad (3.3.5)$$

and then fix the points to the gauge $x_5 = \infty$, $x_1 = (1, 0 \dots 0)$ and $x_2 = 0$. As was mentioned in the earlier section (3.2.1), the Faddeev Popov determinant for this gauge choice is just 1. Hence we get the following expression:

$$I_{\Delta,J} = \int \frac{d^d x_3 d^d x_4}{\text{vol}(\text{SO}(d-1))} \frac{\langle O_1 O_2 O_3 O_4 \rangle}{|x_{34}|^{2d-\Delta_3-\Delta_4-\Delta}} \hat{C}_J\left(\frac{x_{34} \cdot x_{12}}{|x_{34}||x_{12}|}\right) \quad (3.3.6)$$

The gauge we group with whose volume we modulo out the integral changes as we fix the gauge. The initial integral given by (3.3.5) is conformally invariant under the conformal transformations of the four points. In (3.3.6), however the two points are invariant under rotations in the $d-1$ dimensional Euclidean space. Hence, we divide by $\text{SO}(d-1)$.

3.3.2 Resolving the divergences

In the above integral (3.3.6), the angle is measured with respect to the imaginary time axis, i.e x^0 direction. Gegenbauer polynomials for the integration range pertaining to the above integral diverge in every null direction for an integer spin J . What we wish to do is to find an integrand which would not diverge along some particular null direction. To this end, we first write the Gegenbauer polynomials in a particular representation:

$$|x|^J = \hat{C}_J\left(\frac{x^0}{|x|}\right) = \frac{\hat{C}_J(1)}{\text{vol}(S^{d-2})} \int_{S^{d-2}} d^{d-2} \hat{e} (n \cdot x)^J \quad (3.3.7)$$

where $n = (1, i\hat{e})$ is a null vector and \hat{e} is unit vector in $d - 1$ dimensions. Gegenbauer polynomials are symmetric traceless spherical harmonics in higher dimensions, i.e they are analogous to Y_m^l s in three dimensions with $m = 0$. Therefore these are symmetric under ϕ rotations. So once we fix the angle with respect to the chosen axis, rotations about this axis will not affect these Gegenbauer polynomials. Therefore they satisfy:

$$\nabla^2 \hat{C}_J = 0 \quad (3.3.8)$$

We can easily prove that (3.3.7) satisfies the above equation.

Using this representation in (3.3.6), we get:

$$I_{\Delta, J} = \frac{\hat{C}_J(1)}{\text{vol}(S^{d-2})} \int \frac{d^d x_3 d^d x_4}{\text{vol}(\text{SO}(d-1))} \int_{S^{d-2}} d\hat{e} \frac{\langle O_1 O_2 O_3 O_4 \rangle}{|x_{34}|^{J+2d-\Delta_3-\Delta_4-\Delta}} (x_{34} + i\hat{e} \cdot x_{34})^J \quad (3.3.9)$$

In the above equation, we have an integral over the S^{d-2} sphere. Again we fix gauge by choosing $\hat{e} = (0, 1, 0, \dots, 0)$. Fixing this gauge also gives a Faddeev Popov determinant of 1. So no additional factors enter the integral. Doing this leads to the following integral.

$$I_{\Delta, J} = \hat{C}_J(1) = \int \frac{d^d x_3 d^d x_4}{\text{vol}(\text{SO}(d-1))} \frac{\langle O_1 O_2 O_3 O_4 \rangle}{|x_{34}|^{J+2d-\Delta_3-\Delta_4-\Delta}} (x_{34}^0 + ix_{34}^1)^J \quad (3.3.10)$$

The form of this integral seems familiar, since we had encountered an integral of this kind in the two dimensional case. This is the Euclidean inversion formula in higher dimensions. In the next subsection, we will perform a Wick rotation, in a way analogous to the two dimensional case.

Differentiating from the two dimensional case

In the two dimensional case, we did not have to go through this circuitous route of isolating a null direction. There we just got an integrand which did not diverge along all null directions. What was different? As highlighted briefly before, symmetric traceless representations in two dimensions are reducible. This is another way of saying that the Gegenbauer polynomials in two dimensions can be broken down conveniently into two pieces. These two pieces when integrated separately lead to an integrand which is finite and well-behaved. This is precisely equivalent to the fact that we considered just one part of the complete partial wave in two dimensions. The complete wave would have been $\Psi_{h, \bar{h}} + \Psi_{\bar{h}, h}$ and we considered $\Psi_{h, \bar{h}}$. Thus, behind the scenes we had already chucked out the part

which would have rendered our integrand in two dimensions to be divergent in all null directions. This is the reason we were able to proceed in our calculation without considering these nuances we are encountering in the higher dimensional case.

3.3.3 Wick rotation

Once we have the Euclidean inversion formula as mentioned above, we can perform a Wick rotation and get the Lorentzian version. Once again our contour manipulation will closely mirror the detailed analysis done for the 2 dimensional case. Like before, we prefer to work in light-cone coordinates, $u = x^0 + ix^1 = x^0 - t$. The wick rotated axis will be x_1 and will play the role that τ played in the 2 dimensional case - the imaginary time axis. The real time t is defined as $x^1 = it$. Therefore, all our contour manipulation will take place in the x^1 complex plane. Now, in the lightcone coordinates, our integral after having isolated a null direction (3.3.10), converts to:

$$I_{\Delta,J} = -\hat{C}_J(1) \int \frac{d^d x_3 d^d x_4}{\text{vol}(\text{SO}(d-1))} \frac{\langle O_1 O_2 O_3 O_4 \rangle}{x_{34}^{2 \cdot \frac{J+2d-\Delta_3-\Delta_4-\Delta}{2}}} u_{34}^J \quad (3.3.11)$$

We get an extra negative sign when connecting the above formula to (3.3.10), because of the change in the measure - we get two imaginary units i accompanying dx_3^1 and dx_4^1 . As before the above integral cannot be gotten by a simple redefinition of the variables. We need to watch out for the poles of the integrand, specifically the correlator in the complex x^1 plane as perform the contour manipulation.

In this section, we skip the details and refer the reader to section (3.2.2), where the entire contour manipulation has been detailed in its full glory. Appendix (A) also highlights the wick rotation of correlators. Here, after having introduced a null vector $m^\mu = (1, 1, 0, \dots, 0)$ such that $m \cdot x = u$, the final integral in Lorentzian space after performing a Wick rotation is given by :

$$\begin{aligned} I_{\Delta,J} = & -\hat{C}_J(1) \left[(-1)^J \times \right. \\ & \int_{4>1,2>3} \frac{d^d x_3 d^d x_4}{\text{vol}(\text{SO}(d-1))} \frac{\langle [O_3, O_2][O_1, O_4] \rangle}{|x_{34}|^{J+2d-\Delta_3-\Delta_4-\Delta}} (-m \cdot x_{34})^J \theta(-m \cdot x_{34}) \\ & \left. + \int_{3>1,2>4} \frac{d^d x_3 d^d x_4}{\text{vol}(\text{SO}(d-1))} \frac{\langle [O_4, O_2][O_1, O_3] \rangle}{|x_{34}|^{J+2d-\Delta_3-\Delta_4-\Delta}} (m \cdot x_{34})^J \theta(m \cdot x_{34}) \right] \end{aligned} \quad (3.3.12)$$

This formula is now analytic in J and we can see this fact separately for even and odd J .

Here in this formula, we are integrating over two Lorentzian patches. The theta functions in the integral demonstrate the fact that at a time, only one integral will contribute. The regions demarcated by R_1 and R_2 (3.2.17) in the two dimensional case are demarcated through the theta functions in the higher dimensional case, though the principle remains the same. In order to get a non-vanishing contribution to $I_{\Delta,J}$, we need to have the positions of the poles in a specific order. Then, we can push the contours around these branch cuts to generate the double commutators. For the other case, outside of the Lorentzian

patches referred to by the inversion formula, we can close the contour in regions where there are no poles and hence do not contribute to the integral. Also, for both the Lorentzian patches, x_3 and x_4 are space-like separated, therefore we can replace x_{34}^2 with $|x_{34}|$, as has been done in the above formula (3.3.12). For this formula too, the requirement that $J \geq 0$ is not relaxed. In order for the integrals to vanish at infinity, we need J to be an integer and greater than 0. Ensuring this enables us to drop the arcs at infinity, which is necessary for the analysis. However, as evidenced by appendix D.2 of [22], the formula actually holds for $J > 1$.

A few more comments before we on to further. Some of these comments have been made for the two dimensional case, however we paraphrase them shortly to maintain continuity from the physics perspective. In the above integral, the causal relationship between the four points is highlighted by the choice of the Lorentzian patches. This is one instance of the physicality of the entire construct. After having started from a purely complex analysis problem of poles and contour manipulations, we are ending up with a formula that is analytic in J and calculates the CFT parameters of a physical theory. Also, while performing contour rearrangements, we are only worried about the Regge behaviour of u^J and not of the correlator. This is another physical aspect that has to be kept in mind. In fact, according to recent paper by [14], the Regge behaviour of four point functions is not arbitrary. By establishing the chaos bound, no anomalous behaviour of the four point correlator is expected at these Regge limits.

In the two dimensional case, after having done the Wick rotation, we wished to express the result in cross ratio space. Similarly, in this case too, we hope to express 3.3.12 as an integral in the cross ratio space: χ and $\bar{\chi}$ as defined in (2.2.6) and (2.2.7).

3.3.4 In cross ratio terms

To get to the cross ratio space, we need to go through two steps: averaging over the null directions which we had fixed earlier to perform the integral and second, to change the gauge choice we have chosen now.

Covering all null directions

We isolated a null direction in the earlier. Here, we undo that process. After having got the Lorentzian inversion formula which is analytic in J , we can average over the null directions. Note that we had picked up a direction to fix gauge so as to get a formula analogous to the two dimensional case. However, with the present gauge choice with $x_1 = 1$, $x_2 = 0$ and $x_5 = \infty$, we will not be able to get an integral over the cross ratio space. We will have to move to new gauge choice which will be highlighted later. So, for doing this, we need the most general form of the integral in its full glory - including all the gauge invariant terms. Hence, we will have to ungauged fix the whole integral we have in (3.3.12). The first step to doing this would be to re-implement the rotational symmetry in S^{d-2} we had before fixing a particular unit direction in (3.3.9). To do this, in (3.3.24), we need to average over m . Hence, with $g \in \text{SO}(d-2, 1)$,

we get the following equation for averaging over the null directions.

$$\begin{aligned}
I_{\Delta,J} = & -\hat{C}_J(1) \left[(-1)^J \times \right. \\
& \int_{4>1,2>3} \frac{d^d x_3 d^d x_4}{\text{vol}(\text{SO}(d-1))} \frac{< [O_3, O_2][O_1, O_4] >}{|x_{34}|^{J+2d-\Delta_3-\Delta_4-\Delta}} \int_{\text{SO}(d-2,1)} dg(-gm_{34})^J \theta(-gm_{34}) \\
& + \int_{3>1,2>4} \frac{d^d x_3 d^d x_4}{\text{vol}(\text{SO}(d-1))} \frac{< [O_4, O_2][O_1, O_3] >}{|x_{34}|^{J+2d-\Delta_3-\Delta_4-\Delta}} \int_{\text{SO}(d-2,1)} dg(gm_{34})^J \theta(gm_{34}) \left. \right]
\end{aligned} \tag{3.3.13}$$

There are few steps required to connect the dots between the above equation and the final expression gotten (3.3.14) after completing the integration. We will skip these steps and refer the interested reader to section 3.5 of [22]. The final integral is given by:

$$\begin{aligned}
I_{\Delta,J} = & -\frac{\hat{C}_J(1)}{\text{vol}(S^{d-2})} \left[(-1)^J \int_{4>1,2>3} \frac{d^d x_3 d^d x_4}{\text{vol}(\text{SO}(d-2,1))} \frac{< [O_3, O_2][O_1, O_4] >}{|x_{34}|^{J+2d-\Delta_3-\Delta_4-\Delta}} B_J(-\eta) \right. \\
& + \left. \int_{3>1,2>4} \frac{d^d x_3 d^d x_4}{\text{vol}(\text{SO}(d-2,1))} \frac{< [O_4, O_2][O_1, O_3] >}{|x_{34}|^{J+2d-\Delta_3-\Delta_4-\Delta}} B_J(\eta) \right]
\end{aligned} \tag{3.3.14}$$

where $\eta = \frac{x_{12} \cdot x_{34}}{|x_{12}| |x_{34}|}$ and $B_J(\eta)$ is defined as follows:

$$B_J(y) = \frac{\pi^{\frac{d-2}{2}} \Gamma(J+1)}{2^J \Gamma(J+\frac{d}{2})} (1+y)_2^{2-d-J} F_1\left(J+\frac{d-1}{2}, J+d-2, 2J+d-1, \frac{2}{y+1}\right) \tag{3.3.15}$$

Now we will unfix the gauge choice we had made, and choose a gauge that will allow us to write the inversion formula as an integral over just the cross ratios.

New gauge

If we undo the gauge fixing that we did, and write the integral (3.3.14) as an integral over 5 variables, we get the following:

$$\begin{aligned}
I_{\Delta,J} = & -\hat{C}_J(1) \left[(-1)^J \int_{4>1,2>3} \frac{d^d x_1 d^d x_2 d^d x_3 d^d x_4 d^d x_5}{\text{vol}(\text{SO}(d,2))} \frac{< [O_3, O_2][O_1, O_4] >}{|x_{12}|^{\tilde{\Delta}_1+\tilde{\Delta}_2-\tilde{\Delta}} |x_{15}|^{\tilde{\Delta}_1+\tilde{\Delta}-\tilde{\Delta}_2} |x_{25}|^{\tilde{\Delta}_2+\tilde{\Delta}-\tilde{\Delta}_1}} \right. \\
& \times \frac{B_J(-\eta)}{|x_{34}|^{\tilde{\Delta}_3+\tilde{\Delta}_4-\tilde{\Delta}} |x_{35}|^{\tilde{\Delta}_3+\tilde{\Delta}-\tilde{\Delta}_4} |x_{45}|^{\tilde{\Delta}_4+\tilde{\Delta}-\tilde{\Delta}_3}} \\
& + \int_{3>1,2>4} \frac{d^d x_1 d^d x_2 d^d x_3 d^d x_4 d^d x_5}{\text{vol}(\text{SO}(d,2))} \frac{< [O_4, O_2][O_1, O_3] >}{|x_{12}|^{\tilde{\Delta}_1+\tilde{\Delta}_2-\tilde{\Delta}} |x_{15}|^{\tilde{\Delta}_1+\tilde{\Delta}-\tilde{\Delta}_2} |x_{25}|^{\tilde{\Delta}_2+\tilde{\Delta}-\tilde{\Delta}_1}} \\
& \times \frac{B_J(\eta)}{|x_{34}|^{\tilde{\Delta}_3+\tilde{\Delta}_4-\tilde{\Delta}} |x_{35}|^{\tilde{\Delta}_3+\tilde{\Delta}-\tilde{\Delta}_4} |x_{45}|^{\tilde{\Delta}_4+\tilde{\Delta}-\tilde{\Delta}_3}} \left. \right]
\end{aligned} \tag{3.3.16}$$

As before, in the new gauge choice that we will choose, we need to maintain the causal structure of the lorentzian patches that we had in the first gauge. Therefore, x_5 has to be space-like separated from the all the four points. To this end,

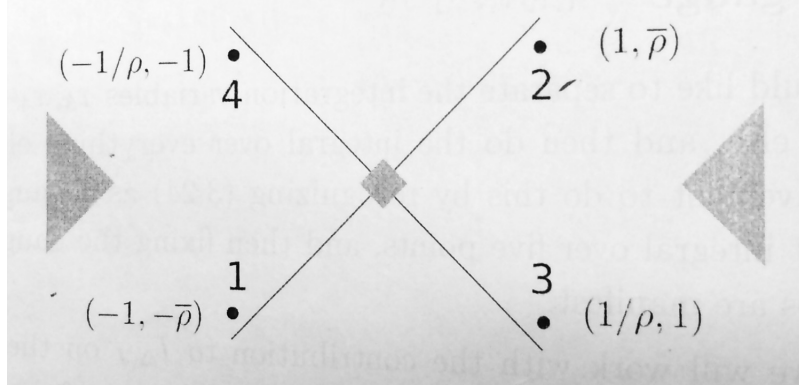


Figure 3.2: Configuration for the 4 points given in lightcone coordinates. This new gauge choice corresponds to the first Lorentzian patch. x_5 is spacelike separated from all 4 points. (Borrowed from [22])

we will pick up a gauge as given in the figure (3.3.4). Here the causal relationship corresponds to the first Lorentzian patch R_1 . The coordinates given in the figure (3.3.4) are lightcone coordinates. It is always possible to use conformal transformations to fix 4 points on the plane. This was proven in (2.2.2). To get to the present configuration, use the $\rho - \chi$ and $\bar{\rho} - \bar{\chi}$ relationship given in (3.3.17).

$$\begin{aligned}\chi &= \frac{4\rho}{(1+\rho)^2} \\ \bar{\chi} &= \frac{4\bar{\rho}}{(1+\bar{\rho})^2}\end{aligned}\tag{3.3.17}$$

To get a better feel of the relationship between the cross ratios in $\chi - \bar{\chi}$ plane and the $\rho - \bar{\rho}$ plane, refer [9].

After having chosen this gauge, we will have an integral in the cross ratio space and a left over integral over x_5 keeping in mind the fact that x_5 is spacelike separated from each of the four points.

3.3.5 Evaluating the hanging integral

In this section, we will focus on integrating out the x_5 variable. After this step, we will have an integral over the 4 points x_1, x_2, x_3 and x_4 .

Isolating out the parts of the integrand dependent on x_5 , we get the following integral:

$$\begin{aligned}H_{\Delta,J}(x_i) &= \int_{\text{spacelike}} d^d x_5 \frac{1}{|x_{12}|^{\bar{\Delta}_1 + \bar{\Delta}_2 - \bar{\Delta}} |x_{15}|^{\bar{\Delta}_1 + \bar{\Delta} - \bar{\Delta}_2} |x_{25}|^{\bar{\Delta}_2 + \bar{\Delta} - \bar{\Delta}_1}} \\ &\quad \times \frac{B_J(-\eta)}{|x_{34}|^{\bar{\Delta}_3 + \bar{\Delta}_4 - \Delta} |x_{35}|^{\bar{\Delta}_3 + \Delta - \bar{\Delta}_4} |x_{45}|^{\bar{\Delta}_4 + \Delta - \bar{\Delta}_3}}\end{aligned}\tag{3.3.18}$$

We are considering just the first Lorentzian patch R_1 and hence refer to the configuration given in figure (3.3.4) to determine the integration range with x_5 being spacelike separated from these four points.

The entire calculation is skipped in this section and the interested reader is referred to [22] for a detailed derivation. Here we will mention some salient features of the integration and move on towards our final result.

Firstly, the integral (3.3.18) is similar to the conformal partial wave we defined earlier in (2.4.3), with the external dimensions of the four operators being $\tilde{\Delta}_1, \tilde{\Delta}_2, \tilde{\Delta}_3$ and $\tilde{\Delta}_4$ and the running dimension being $\tilde{\Delta}$. This is because we are just opening up the three point function present inside the integral. Hence, this integral is conformally invariant. Now, this expression can be cleaned up into a part solely dependent on the cross ratios χ and $\bar{\chi}$ and a part dependent on the coordinates. This is analogous to the way we did for the four point function in (2.2.5). Hence we get the following :

$$H_{\Delta,J}(x_i) = T^{\tilde{\Delta}_i}(x_i) H_{\Delta,J}(\chi, \bar{\chi}) = \frac{1}{|x_{12}|^{2d} |x_{34}|^{2d}} \frac{1}{T^{\tilde{\Delta}_i}(x_i)} H_{\Delta,J}(\chi, \bar{\chi}) \quad (3.3.19)$$

where

$$T^{\tilde{\Delta}_i}(x_i) = \frac{1}{|x_{12}|^{\Delta_1+\Delta_2} |x_{34}|^{\Delta_3+\Delta_4}} \left(\frac{|x_{14}|}{|x_{24}|} \right) \left(\frac{|x_{14}|}{|x_{13}|} \right) \quad (3.3.20)$$

Here we will use the modulus sign for x_{14} and x_{23} even though they are timelike separated in the Lorentzian patch R_1 we are interested in. This is because we expect the integral $H_{\Delta,J}$ to be real, since we are integrating over physical coordinates in Lorentzian space.

Secondly, we can determine the behaviour of Casimir equations by assuming the small $\chi, \bar{\chi}$ limit. We will not go into the nuances of this procedure. But the important point is that by solving the integral in this limit, we can guess the nature of the final expression for $H_{\Delta,J}$. Here we will just mention the final result of the integration:

$$H_{\Delta,J}(\chi, \bar{\chi}) = a_{\Delta,J} G_{J+d-1, \Delta-d+1}^{\tilde{\Delta}_i}(\chi, \bar{\chi}) \quad (3.3.21)$$

where

$$a_{\Delta,J} = \frac{(2\pi)^{d-2}}{2} \times \frac{\Gamma(J+1) \Gamma(\Delta - \frac{d}{2}) \Gamma(\frac{\Delta_{12}+J+\Delta}{2}) \Gamma(\frac{\Delta_{21}+J+\Delta}{2}) \Gamma(\frac{\Delta_{34}+J+\tilde{\Delta}}{2}) \Gamma(\frac{\Delta_{43}+J+\tilde{\Delta}}{2})}{\Gamma(J + \frac{d}{2}) \Gamma(\Delta - 1) \Gamma(J + \Delta) \Gamma(J + d - \Delta)} \quad (3.3.22)$$

Once we have this expression, we are only left with an integral over the four coordinates corresponding to the external operators. The next section will highlight why needed this new gauge after all. The old gauge would not have given us an integral over the cross ratio space. This new gauge does.

3.3.6 Integral over cross ratios

The integral over the four points can be rewritten in terms of just the cross ratios. Following the calculation from the previous section, (3.3.16) converts

into:

$$\begin{aligned}
I_{\Delta,J} = & -\frac{\hat{C}_J(1)}{\text{vol}(S^{d-2})} \left[(-1)^J \times \right. \\
& \int_{4>1,2>3} \frac{d^d x_1 d^d x_2 d^d x_3 d^d x_4}{\text{vol}(\text{SO}(d,2))} < [O_3, O_2][O_1, O_4] > H_{\Delta,J}(\chi, \bar{\chi}) \\
& \left. + \int_{3>1,2>4} \frac{d^d x_1 d^d x_2 d^d x_3 d^d x_4}{\text{vol}(\text{SO}(d,2))} < [O_4, O_2][O_1, O_3] > H_{\Delta,J}(\chi, \bar{\chi}) \right]
\end{aligned} \tag{3.3.23}$$

We now fix gauge (3.3.4) and move into the cross ratio space. Accounting for the Faddeev Popov determinant due to the choice of orbit and the Jacobian corresponding to the change of variables from $\rho - \bar{\rho}$ space to the $\chi - \bar{\chi}$ space, we finally end up with the following expression:

$$\begin{aligned}
I_{\Delta,J} = & \alpha_{\Delta,J} \left[(-1)^J \times \right. \\
& \int_0^1 \int_0^1 \frac{d\chi d\bar{\chi}}{(\chi\bar{\chi})^d} |\chi - \bar{\chi}|^{d-2} G_{J+d-1, \Delta-d+1}^{\tilde{\Delta}_i}(\chi, \bar{\chi}) \frac{< [O_3, O_2][O_4, O_1] >}{T^{\Delta_i}} \\
& \left. + \int_{-\infty}^0 \int_{-\infty}^0 \frac{d\chi d\bar{\chi}}{(\chi\bar{\chi})^d} |\chi - \bar{\chi}|^{d-2} G_{J+d-1, \Delta-d+1}^{\tilde{\Delta}_i}(\chi, \bar{\chi}) \frac{< [O_4, O_2][O_1, O_3] >}{T^{\Delta_i}} \right]
\end{aligned} \tag{3.3.24}$$

where

$$\alpha_{\Delta,J} = -\frac{a_{\Delta,J}}{2^d} \frac{\hat{C}_J(1)}{\text{vol}(\text{SO}(d-1))} \tag{3.3.25}$$

and $a_{\Delta,J}$ has been defined in (3.3.22). Equation (3.3.24) is the final expression, we had sought out to look for. We wanted to find an expression which would allow us to calculate the parameters of the CFT data by performing a conformally invariant integral in cross-ratio space over two Lorentzian patches. This is precisely what we get through this equation.

This is an elegant way of getting the CFT parameters. Simon Caron-Huot in his seminal paper [3] got the double commutator by performing an analytic continuation in the cross-ratio space rather than in the coordinate space. We now show that performing an analytic continuation in cross ratio space gives rise to the double commutator.

3.3.7 Analytic continuation in cross-ratio space

Consider the configuration given in (3.3.4). As highlighted in appendix (A) an Euclidean integral corresponds to all the four points being space-like separated from each other. To move into Lorentzian space, we need to make some combination of these four points into locations such that two pairs of these are time-like separated; in this case $4>1$ and $2>3$. In appendix (A), we have given a general method of analytically continuing correlators in Euclidean theory to Lorentzian theory. We will use the techniques highlighted there to get the double commutator by performing the analytic continuation of a four point function in cross-ratio space rather than in Minkowski spacetime. Therefore in Euclidean space a four point function is given by (2.2.5) and we wish to perform an analytic continuation in the $\chi - \bar{\chi}$ plane

The first thing to do would be analyse when (4,1) and (2,3) will move from being spacelike separated to being timelike separated. In fact we are searching for a point when the two pairs will become lightlike separated. This transition will imply a transition from the Euclidean spacetime to Minkowski spacetime. Therefore, following from (3.2.12), we get:

$$x_{14}^2 = x_{23}^2 = (1 - \frac{1}{\rho})(\bar{\rho} - 1) \quad (3.3.26)$$

For timelike separation:

$$\begin{aligned} x_{14}^2 = x_{23}^2 < 0 &\implies (1 - \frac{1}{\rho})(\bar{\rho} - 1) < 0 \\ &\implies \rho > 1 \text{ and } \bar{\rho} > 1 \end{aligned} \quad (3.3.27)$$

Similarly for spacelike separation:

$$\begin{aligned} x_{14}^2 = x_{23}^2 > 0 &\implies (1 - \frac{1}{\rho})(\bar{\rho} - 1) > 0 \\ &\implies \rho > 1 \text{ and } \bar{\rho} < 1 \end{aligned} \quad (3.3.28)$$

We will concern ourselves just with the movement of $\bar{\rho}$, keeping ρ fixed. The cross ratios defined in (2.2.7) can be written in terms of lightcone coordinates in the following way:

$$\begin{aligned} \chi &= \frac{u_{21}u_{34}}{u_{31}u_{24}} \\ \bar{\chi} &= \frac{v_{21}v_{34}}{v_{31}v_{24}} \end{aligned} \quad (3.3.29)$$

We will first concern ourselves with how the analytic continuation affects the $g(\chi, \bar{\chi})$ part. We will then move on to study the effects on the spacetime dependent parts.

Correlator $\langle O_1 O_4 O_2 O_3 \rangle$

Consider the correlator $\langle O_1 O_4 O_2 O_3 \rangle$. Following the analysis done in appendix (A), we can say the following:

$$t_i \rightarrow t_i - i\epsilon_i \text{ with } \epsilon_1 > \epsilon_4 > \epsilon_2 > \epsilon_3 \quad (3.3.30)$$

This implies that:

$$\begin{aligned} t_{23} &\rightarrow t_{23} - i\epsilon \\ t_{14} &\rightarrow t_{14} - i\epsilon \\ &\text{with } \epsilon > 0 \end{aligned} \quad (3.3.31)$$

Therefore:

$$(1 - \bar{\chi}) = \frac{v_{32}v_{14}}{v_{31}v_{24}} \quad (3.3.32)$$

From (3.3.31) and the definition of lightcone coordinates, we get:

$$(1 - \bar{\chi}) = \frac{(v_{32} + i\epsilon)(v_{14} - i\epsilon)}{v_{31}v_{24}} \quad (3.3.33)$$

Converting to $\rho - \bar{\rho}$ coordinates and we get:

$$\begin{aligned}
(1 - \bar{\chi}) &= \frac{(1 - \bar{\rho} + i\epsilon)(1 - \bar{\rho} - i\epsilon)}{(\bar{\rho} + 1)(\bar{\rho} + 1)} \\
&= \frac{(1 - \bar{\rho})^2 + \epsilon^2}{(\bar{\rho} + 1)^2} > 0 \\
&\implies \bar{\chi} < 1
\end{aligned} \tag{3.3.34}$$

If we look at the figure (3.3.7), we see the $\bar{\chi}$ plane. $\bar{\chi} < 0$ does not intersect any branch point and so the contour will be entrapped in the $|\bar{\chi}| < 1$ range. We can see that an analytic continuation of this correlator would not affect $g(\chi, \bar{\chi})$, since we do not cross any branch cuts.

Correlator $\langle O_1 O_4 O_3 O_2 \rangle$

Now consider the correlator $\langle O_1 O_4 O_3 O_2 \rangle$. Therefore, in a manner analogous to the method discussed above:

$$\begin{aligned}
t_{32} &\rightarrow t_{32} - i\epsilon \\
t_{14} &\rightarrow t_{14} - i\epsilon \\
&\text{with } \epsilon > 0
\end{aligned} \tag{3.3.35}$$

Therefore:

$$\begin{aligned}
(1 - \bar{\chi}) &= \frac{v_{32}v_{14}}{v_{31}v_{24}} = \frac{(v_{32} - i\epsilon)(v_{14} - i\epsilon)}{v_{31}v_{24}} \\
&= \frac{(1 - \bar{\rho} - i\epsilon)(1 - \bar{\rho} - i\epsilon)}{(\bar{\rho} + 1)(\bar{\rho} + 1)} \\
&= \frac{(1 - \bar{\rho})^2 - 2i\epsilon(1 - \bar{\rho})}{(1 + \bar{\rho})}
\end{aligned} \tag{3.3.36}$$

Since we want to go from (3.3.28) to (3.3.27), we move from $\bar{\rho} < 1$ to $\bar{\rho} > 1$. Therefore we can use $\bar{\rho} = 1 - \delta$. Hence, (3.3.36) converts into:

$$\begin{aligned}
1 - \bar{\chi} &= \frac{(\delta - i\epsilon)^2}{(1 + 1 - \delta)^2} \\
&= \frac{1}{4}(\delta - i\epsilon)^2 \left(1 - \frac{\delta}{2}\right)^{-2} \\
&= \frac{1}{4}(\delta^2 - 2i\delta\epsilon)
\end{aligned} \tag{3.3.37}$$

Moving from $\bar{\rho} < 1$ to $\bar{\rho} > 1$ is equivalent to moving from $\delta > 0$ to $\delta < 0$.

$$\begin{aligned}
\delta < 0; \bar{\rho} > 1; \text{Im}(1 - \bar{\chi}) > 0 &\implies \text{Im}(\bar{\chi}) < 0 \\
\delta > 0; \bar{\rho} < 1; \text{Im}(1 - \bar{\chi}) < 0 &\implies \text{Im}(\bar{\chi}) > 0
\end{aligned} \tag{3.3.38}$$

Thus, the this correlator gives rise to a clockwise rotation of $g(\chi, \bar{\chi})$ about $\bar{\chi} = 1$. This has been highlighted in figure (3.3.7).

For these two correlators, $t_{14} \rightarrow t_{14} - i\epsilon$, therefore we get:

$$\begin{aligned}
x_{14}^2 &= -t_{14}^2 + \dots \\
&= -(t_{14} - i\epsilon)^2 \\
&= \dots - i\epsilon \text{ since } t_1 < t_4
\end{aligned} \tag{3.3.39}$$

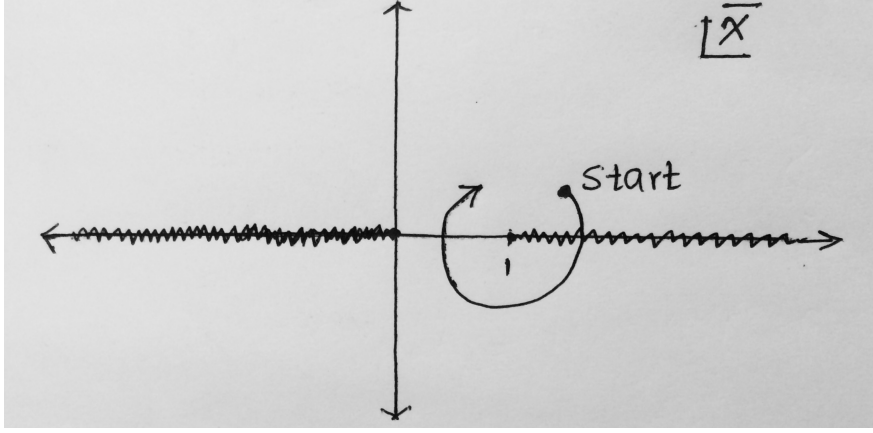


Figure 3.3: Complex $\bar{\chi}$ plane. Clockwise rotation about $\bar{\chi} = 1$ corresponds to the analytic continuation of $g(\chi, \bar{\chi})$

If we refer to the prefactor accompanying $g(\chi, \bar{\chi})$ in (2.2.5), using the above expression, we get an additional factor of $(e^{-i\pi})^{\frac{\Delta_2 - \Delta_1}{2} + \frac{\Delta_3 - \Delta_4}{2}}$. For the other two correlators, $\langle O_4 O_1 O_2 O_3 \rangle$ and $\langle O_4 O_1 O_3 O_2 \rangle$, we will get a contribution of $(e^{+i\pi})^{\frac{\Delta_2 - \Delta_1}{2} + \frac{\Delta_3 - \Delta_4}{2}}$. We will not go into the details for analytically continuing $g(\chi, \bar{\chi})$ for these two correlators. We will just summarise the results below.

$$\begin{aligned}
\langle O_1 O_4 O_2 O_3 \rangle &: e^{-i\pi \frac{\Delta_2 - \Delta_1 + \Delta_3 - \Delta_4}{2}} \times g(\chi, \bar{\chi}) \\
\langle O_1 O_4 O_3 O_2 \rangle &: e^{-i\pi \frac{\Delta_2 - \Delta_1 + \Delta_3 - \Delta_4}{2}} \times g^\odot(\chi, \bar{\chi}) \\
\langle O_4 O_1 O_2 O_3 \rangle &: e^{i\pi \frac{\Delta_2 - \Delta_1 + \Delta_3 - \Delta_4}{2}} \times g^\odot(\chi, \bar{\chi}) \\
\langle O_4 O_1 O_3 O_2 \rangle &: e^{i\pi \frac{\Delta_2 - \Delta_1 + \Delta_3 - \Delta_4}{2}} \times g(\chi, \bar{\chi})
\end{aligned} \tag{3.3.40}$$

Thus analytically continuing (2.2.5) and removing out the normalisation factor T^{Δ_1} defined in (3.3.20), we get the following (where we define the double discontinuity) :

$$\begin{aligned}
\frac{\langle [O_3 O_2][O_1, O_4] \rangle}{T^{\Delta_i}} &= -2\cos(\pi \frac{\Delta_2 - \Delta_1 + \Delta_3 - \Delta_4}{2})g(\chi, \bar{\chi}) + e^{i\pi \frac{\Delta_2 - \Delta_1 + \Delta_3 - \Delta_4}{2}}g^\odot(\chi, \bar{\chi}) \\
&+ e^{-i\pi \frac{\Delta_2 - \Delta_1 + \Delta_3 - \Delta_4}{2}}g^\odot(\chi, \bar{\chi}) \\
&= -2\text{dDisc}[g(\chi, \bar{\chi})]
\end{aligned} \tag{3.3.41}$$

This was for the first Lorentzian patch, where we have contour rotations about $\bar{\chi} = 1$. For the second Lorentzian patch, the contour manipulation would be taking a path around $\bar{\chi} = \infty$ and we get a similar expression as the one above:

$$\begin{aligned}
\frac{\langle [O_4 O_2][O_1, O_3] \rangle}{T^{\Delta_i}} &= -2\cos(\pi \frac{\Delta_2 - \Delta_1 + \Delta_4 - \Delta_3}{2})g(\chi, \bar{\chi}) + e^{i\pi \frac{\Delta_3 - \Delta_4 + \Delta_2 - \Delta_1}{2}}g^\odot(\chi, \bar{\chi}) \\
&+ e^{-i\pi \frac{\Delta_3 - \Delta_4 + \Delta_2 - \Delta_1}{2}}g^\odot(\chi, \bar{\chi}) \\
&= -2\text{dDisc}[g(\chi, \bar{\chi})]
\end{aligned} \tag{3.3.42}$$

So, here we have shown that an analytic continuation of the four point correlator in cross ratio space also gives rise to the double commutator. This also connects the forms of the final result as given in [3] and [22].

In the next chapter, we will give a derivation of the inversion formula the way Caron-Huot proved it. We will see how the spacetime derivation differs from it and whether there are any fundamental differences in physics in the two approaches.

Chapter 4

Cross-Ratio Derivation

This method of getting to the inversion formula was formulated in the paper [3]. In this chapter, we will go through this derivation. We will see some of its salient features; in particular how it differs from the spacetime derivation method explained in the previous chapter.

4.1 Introduction

We first set down some notation. In (2.3.9) and (2.3.8), we were dealing with operators having the same scaling dimension. The modification and a light change in notation is given through the following set of equations.

$$\begin{aligned}
 \langle O_1 O_2 O_3 O_4 \rangle &= \frac{1}{(x_{12}^2)^{\frac{\Delta_1+\Delta_2}{2}} (x_{34}^2)^{\frac{\Delta_3+\Delta_4}{2}}} \left(\frac{x_{14}^2}{x_{24}^2} \right)^{\frac{\Delta_1-\Delta_2}{2}} \left(\frac{x_{14}^2}{x_{13}^2} \right)^{\frac{\Delta_3-\Delta_4}{2}} g(u, v) \\
 g(u, v) &= \sum_{J, \Delta} f_{12O} f_{43O} G_{J, \Delta}(\chi, \bar{\chi}) \\
 G_{\Delta, J}^{\Delta_i}(x_i) &= \frac{1}{(x_{12}^2)^{\frac{\Delta_1+\Delta_2}{2}} (x_{34}^2)^{\frac{\Delta_3+\Delta_4}{2}}} \left(\frac{x_{14}^2}{x_{24}^2} \right)^{\frac{\Delta_1-\Delta_2}{2}} \left(\frac{x_{14}^2}{x_{13}^2} \right)^{\frac{\Delta_3-\Delta_4}{2}} G_{J, \Delta}(\chi, \bar{\chi})
 \end{aligned} \tag{4.1.1}$$

In the earlier approach - the spacetime derivation, we started out by expressing the four point correlator as an expansion in the principle series representation. Here we will expand the stripped conformal block $G_{J, \Delta}(\chi, \bar{\chi})$ (after having removed the parts that cannot be expressed in cross-ratio terms from the conformal block) in the principle series representation. We will skip some steps which have been elucidated in detail in the earlier method.

Adopting the notation from (2.2.5), the paper [4] proved the following fact:

$$g(\chi, \bar{\chi}) = 1_{12} 1_{34} + \sum_{J=0}^{\infty} \int_{\frac{d}{2}-i\infty}^{\frac{d}{2}+i\infty} \frac{d\Delta}{2\pi i} c(J, \Delta) F_{J, \Delta}(\chi, \bar{\chi}) \tag{4.1.2}$$

Here the first term corresponds to the identity exchange between the two OPE expansions. From equations (2.3.4) and (2.3.5), we can clearly see the identity exchange term appearing. Also, $F_{J, \Delta}(\chi, \bar{\chi})$ is defined in a manner analogous to

the conformal partial wave from equation (2.4.4):

$$F_{J,\Delta}(\chi, \bar{\chi}) = \frac{1}{2} \left(G_{J,\Delta}(\chi, \bar{\chi}) + \frac{K_{J,d-\Delta}}{K_{J,\Delta}} G_{J,\Delta}(\chi, \bar{\chi}) \right) \quad (4.1.3)$$

where the coefficients are given by:

$$\begin{aligned} K_{\Delta,J} &= \frac{\Gamma((\Delta-1))}{\Gamma(\Delta-\frac{d}{2})} \kappa_{J+\Delta} \\ \kappa_\beta &= \frac{\Gamma(\frac{\beta}{2}-a)\Gamma(\frac{\beta}{2}+a)\Gamma(\frac{\beta}{2}-b)\Gamma(\frac{\beta}{2}+b)}{2\pi^2\Gamma(\beta-1)\Gamma(\beta)} \end{aligned} \quad (4.1.4)$$

where

$$\begin{aligned} a &= \frac{1}{2}(\Delta_1 - \Delta_2) \\ b &= \frac{1}{2}(\Delta_3 - \Delta_4) \end{aligned} \quad (4.1.5)$$

To see a more lucid connection to the conformal partial wave we defined in chapter (2), please refer to [20].

Before moving on, we would like to make some comments regarding the expansion of $g(\chi, \bar{\chi})$. Note that the principal series representation forms a basis of the eigenspace of the eigenfunctions with an eigenvalue of $\Delta(d-\Delta)+J(J+d-2)$. This condition only holds if the operator, in this case the conformal Casimir is self-adjoint. This fact follows from the spectral theorem, which states that an orthonormal basis (a diagonalizable condition) exists for an operator if its self-adjoint. The spectral theorem provides a canonical decomposition. Thus we need to ensure that the operator is self adjoint. As is mentioned in section 3.1 of [3], only when acting on single-valued complex functions will the Casimir operator be self-adjoint. We had used the condition of single-valuedness to impose the condition that we started with an integral spin in chapter (3). We will impose this condition on the spin in this approach too. This will ensure the single-valuedness of $F_{J,\Delta}$, which in turn will ensure that the spectral theorem holds good.

We will now interest ourselves with the primary problem of getting the coefficients $c(J, \Delta)$ by inverting the equation (4.1.2). We will show in the next section why this coefficient contains information about the CFT parameters. The essence of the entire enterprise remains the same - we want to get information about the conformal parameters from complex analysis. The only difference in approaching the problem by this method will be the step where we analytically continue to Lorentzian spacetime. We will talk more about this later.

4.2 Inverting the formula

As we saw in (2.5.1), $F(J, \Delta)$ also form an orthonormal basis. Thus inverting (4.1.2), we get the following expression:

$$c(J, \Delta) = N(J, \Delta) \int d^2\chi \mu(\chi, \bar{\chi}) F_{J,\Delta}(\chi, \bar{\chi}) g(\chi, \bar{\chi}) \quad (4.2.1)$$

where

$$N(J, \Delta) = \frac{\Gamma(J + \frac{d-2}{2})\Gamma(J + \frac{d}{2})K_{J,\Delta}}{2\pi\Gamma(J+1)\Gamma(J+d-2)K_{J,d-\Delta}} \quad (4.2.2)$$

and

$$\mu(\chi, \bar{\chi}) = \left| \frac{\chi - \bar{\chi}}{\chi \bar{\chi}} \right|^{d-2} \frac{((1-\chi)(1-\bar{\chi}))^{a+b}}{(\chi \bar{\chi})^2} \quad (4.2.3)$$

To see how we invert this equation please refer to appendix A of [3].

Operator insertions

In all of our analysis, we will be working in terms of cross ratios. So it will do us good if we fix our four points in a particular gauge. We know that from previous analysis that any four points can be mapped to a plane via 4 conformal transformations. For our purposes, we will fix our configuration as given in figure (3.3.4). This is the first Lorentzian patch R_1 as was described in the first chapter. This Lorentzian patch corresponds to the t channel. We can also fix our configuration in according to the Lorentzian patch R_2 and this will correspond to the u channel. This notationn of the t and u channel corresponds to the Froissart Gribov formula in S-matrix theory, which was the primary motivation as to what led Caron-Huot to come up with the conformal Froissart Gribov approach to get the Lorentzian Inversion formula.

Connecting the CFT parameters with $c(J, \Delta)$

If we look at the OPE expansion of $g(\chi, \bar{\chi})$ from (4.1.1) and compare it with the result (4.1.2), we see that the two formulae would have a semblance with respect to each other if the following equation holds:

$$c_{J,\Delta} = -\text{Res}_{\Delta'=\Delta} c(J', \Delta') \quad (4.2.4)$$

This is because, if we look at the integral in (4.1.2), the possible origin of poles would be the harmonic function and the coefficient function $c(J, \Delta)$. We will consider the poles of the harmonic function in a little while. For now, just consider the ones that originate from $c(J, \Delta)$. The conformal block $G_{J,\Delta}$ vanishes exponentially at large Δ , analogous to the power law $|\rho|^\Delta$. So, in order to perform the integral in (4.1.2), we need to perform the contour manipulation separately for the two distinct parts of the harmonic function $F_{J,\Delta}$. This is in order to keep the integrand well behaved. Therefore, keeping in mind the exponential nature of $G_{J,\Delta}$, for the conformal block, we close the contour towards the right and for the shadow block, we close it towards the left. This is the way we pick up the poles and their respective residues corresponding to $c(J, \Delta)$. Thus, we the residues of the poles of the function $c(J, \Delta)$ are equal to the parameters present in the OPE expansion. This is great. Seemingly by performing an integral of the form (4.1.2), we are able to encode the data corresponding to a conformal field theory within the poles of its integrand. This is the connection, we had alluded to in (3.1), as to how we could encode the CFT data in an integral.

In the above analysis, we have not considered the poles coming from the block itself. So, do these poles exist and if they do, how do they contribute to the residue structure of the integral? Many of these nuances are dealt with in much

more detail in [3] and we refer the reader to this paper for further elucidation on many of these questions. Also, for a better understanding of the poles coming from the conformal blocks, please refer [10] and [11]. We will not delve into these details in this review, but just mention that the residues corresponding to the poles of the conformal block are proportional to the conformal block $G_{J-1-m, J+d-1}$. How this fact ties itself to the residue structure of (4.1.2), will however be referred to some of the papers mentioned above.

4.3 Wick rotation

Once we have the Euclidean inversion formula in (4.2.1), we can perform a Wick rotation to move the integral into Lorentzian space. When we say an analytic continuation, we mean that we move the points from where all of them are spacelike separated from each other a configuration as given in (3.3.4)-where $4 > 1$ and $2 > 3$ are timelike separated and the rest remain spacelike separated. This will again be the most difficult part of the exercise as was the case in the spacetime derivation, and we will have to take care of the singularities arising in the complex plane we perform the analytic continuation in. Also, as opposed to the analytic continuation in Minkowski space we did in the earlier chapter, in this method of deriving the formula, we will analytically continue in the cross ratio $\rho - \bar{\rho}$ space. First we will show the origin of the double discontinuity and then we will perform the complete analytical continuation by moving to new set of coordinates σ and ω . Then we will combine these results to arrive at a final Lorentzian inversion formula.

4.3.1 Double Discontinuity

To get the double discontinuity in the $\rho - \bar{\rho}$ space, we will borrow some ideas from (3.3.7). We will implement the $i\epsilon$ prescription in the $\rho - \bar{\rho}$ space and compare the corresponding prescription in the $\chi - \bar{\chi}$ space done in section (3.3.7) and then match the correlators from (3.3.40).

$$\begin{aligned} \frac{4\bar{\rho}}{(1+\bar{\rho})^2} &\rightarrow \frac{4(\bar{\rho} + i\epsilon)}{(1+\bar{\rho} + i\epsilon)^2} \\ &= \frac{4\bar{\rho}}{(1+\bar{\rho})^2} \left(1 - 2 \times \frac{i\epsilon}{1+\bar{\rho}} \right) \\ &= \frac{4\bar{\rho}}{(1+\bar{\rho})^2} + \frac{4\bar{\rho}(\bar{\rho})}{(1+\bar{\rho})^3} i\epsilon \end{aligned} \quad (4.3.1)$$

To move from spacelike separation (Euclidean theory) to timelike separation (Lorentzian space), we move from $\bar{\rho} < 1$ to $\bar{\rho} > 1$. Hence from the last line of equation (4.3.1) given above, we have the following:

$$\bar{\chi} \rightarrow \chi + \frac{4\bar{\rho}(\bar{\rho})}{(1+\bar{\rho})^3} i\epsilon \quad (4.3.2)$$

Since we move from $\bar{\rho} < 1$ to $\bar{\rho} > 1$, we move from a negative imaginary part to a positive imaginary part. This equals an anticlockwise rotation. On the other hand if we start the analysis in (4.3.1) with a $-\epsilon$ instead of $i\epsilon$, we would move from a positive imaginary part to a negative imaginary part. This corresponds

to a clockwise rotation. Now, if we match these elementary calculations with (3.3.40).

$$\begin{aligned}
\langle O_1 O_4 O_2 O_3 \rangle &: e^{-i\pi \frac{\Delta_2 - \Delta_1 + \Delta_3 - \Delta_4}{2}} \times g(\rho, \bar{\rho}) \\
\langle O_1 O_4 O_3 O_2 \rangle &: e^{-i\pi \frac{\Delta_2 - \Delta_1 + \Delta_3 - \Delta_4}{2}} \times g(\rho, \bar{\rho} - i\epsilon) \\
\langle O_4 O_1 O_2 O_3 \rangle &: e^{i\pi \frac{\Delta_2 - \Delta_1 + \Delta_3 - \Delta_4}{2}} \times g(\rho, \bar{\rho} + i\epsilon) \\
\langle O_4 O_1 O_3 O_2 \rangle &: e^{i\pi \frac{\Delta_2 - \Delta_1 + \Delta_3 - \Delta_4}{2}} \times g(\rho, \bar{\rho})
\end{aligned} \tag{4.3.3}$$

Using these set of equations, the double discontinuity $\text{dDisc}[g(\rho, \bar{\rho})]$ is given by the following result:

$$\begin{aligned}
\text{dDisc}[g(\rho, \bar{\rho})] &= \cos(\pi(a+b))g(\rho, \bar{\rho}) - \frac{1}{2}e^{i\pi(a+b)}g(\rho, \bar{\rho} - i\epsilon) - \frac{1}{2}e^{-i\pi(a+b)}g(\rho, \bar{\rho} + i\epsilon) \\
&= -\frac{1}{2} \langle [O_2, O_3][O_1, O_4] \rangle
\end{aligned} \tag{4.3.4}$$

. Now that we have defined the double discontinuity in $\rho - \bar{\rho}$ space and shown its equivalence to its analog in $\chi - \bar{\chi}$ space, we can move on to redefining the integral in σ and ω coordinates. Before going to that section, we will first talk about monodromies which will be important later.

4.3.2 The Monodromies

Our aim at the end of the day will be to perform an analytical continuation in cross ratio space to get a Lorentzian inversion formula. To this end, We have resolved this issue for the $g(\rho, \bar{\rho})$ part of the integral (4.2.1). The part that remains is the harmonic function which is a sum of the conformal block and its shadow. Analytically continuing these blocks is not straightforward. As was seen in the previous chapter, analytical continuation in the complex plane requires contour manipulations and a major component that played a role back there was the dying out of the integral at large values of v_i . We had a simple polynomial relationship at large v_i which we could use to guess that the arcs at infinity would drop out. This is not the case here. In order to do this, we need another basis of solutions to the quadratic and quartic conformal Casimirs in terms of which these harmonic functions could be written. This basis should have a polynomial divergence/convergence in the areas we are interested in working in. This is what we intend to do in this section - highlight this basis of functions and show how they behave under analytic continuation.

We have mentioned this fact before, but never felt the need to explain it in detail. The quadratic and quartic Casimirs operators are given by:

$$\begin{aligned}
C_2 &= D_z + D_{\bar{z}} + (d-2) \frac{z\bar{z}}{z-\bar{z}} [(1-z)\partial_z - (1-\bar{z})\partial_{\bar{z}}] \\
C_4 &= \left(\frac{z\bar{z}}{z-\bar{z}} \right)^{d-2} (D_z - D_{\bar{z}}) \left(\frac{z\bar{z}}{z-\bar{z}} \right)^{2-d} (D_z - D_{\bar{z}})
\end{aligned} \tag{4.3.5}$$

where the differential operator is given by:

$$D_z = z^2 \partial_z (1-z) \partial_z - (a+b) z^2 \partial_z - abz \tag{4.3.6}$$

and the eigenvalues corresponding to these Casimir operators are:

$$\begin{aligned} c_2 &= \frac{1}{2}[J(J+d-2) + \Delta(d-\Delta)] \\ c_4 &= J(J+d-2)(\Delta-1)(\Delta-d+1) \end{aligned} \quad (4.3.7)$$

We are interested in working in the limit $0 \ll \chi \ll \bar{\chi} \ll 1$. So we need eigenfunctions of the operators mentioned in (4.3.5) with eigenvalues (4.3.7) which behave like power laws in the aforementioned limit:

$$g_{J,\Delta}^{\text{pure}}(\chi, \bar{\chi}) = \chi^{\frac{\Delta-J}{2}} \bar{\chi}^{\frac{\Delta+J}{2}} \times (1 + \text{integer powers of } \chi/\bar{\chi}, \bar{\chi}) \quad (4.3.8)$$

Due to the symmetry of the eigenvalues (4.3.7) of the operators given in (4.3.5), we have 8 independent solutions. These 3 independent Z_2 symmetries are given below:

$$\begin{aligned} J &\leftrightarrow 2-d-J \\ \Delta &\leftrightarrow d-\Delta \\ \Delta &\leftrightarrow 1-J \end{aligned} \quad (4.3.9)$$

Using the behaviour of these solutions in the $\chi, \bar{\chi} \rightarrow 0$ limit and the behaviour of Gegenbauer polynomials, we can express $G_{J,\Delta}$ as a sum of these solutions. We will not go into these details here but the interested reader can refer to section A.1 of [3].

$$G_{J,\Delta}(\chi, \bar{\chi}) = g_{J,\Delta}^{\text{pure}}(\chi, \bar{\chi}) + \frac{\Gamma(J+d-2)\Gamma(-J-\frac{d-2}{2})}{\Gamma(J+\frac{d-2}{2})\Gamma(-J)} g_{-J-d+2,\Delta}^{\text{pure}}(\chi, \bar{\chi}) \quad (4.3.10)$$

There are three regions we will particularly require while performing the analytical continuation. First, would be an anticlockwise rotation about $\bar{\chi} = 1$. Second, a transition from χ to $\bar{\chi}$. And lastly, an anticlockwise rotation around $\chi = 1$. The behaviour of the pure conformal block will depend on the effect the monodromies have when they act on it. More specifically, these pure conformal blocks in two dimensions are hypergeometric functions. So, analysing their behaviour as $\chi \rightarrow 0$ or $\chi \rightarrow 1$ can lead to a mixing of these 8 independent solutions that have been outlined above. The exact mathematics of these monodromies will be skipped in this section and we will just mention the final results and refer the interested reader to appendix A of [3].

Expansion around $z \rightarrow 0$ gives the following result if $g(\chi, \bar{\chi})$ is analytically continued by taking $\bar{\chi}$ in an anticlockwise direction about $\bar{\chi} = 1$. This equation is familiar from section (3.3.7) where we had defined a similar entity.

$$\begin{aligned} g_{J,\Delta}^{\text{pure}\odot} &= g_{J,\Delta}^{\text{pure}}(\chi, \bar{\chi}) \left[1 - 2i \frac{e^{-i\pi(a+b)}}{\sin(\pi(J+\Delta))} \sin(\pi(\frac{J+\Delta}{2} + a)) \sin(\pi(\frac{J+\Delta}{2} + b)) \right] \\ &\quad - \frac{i}{\pi} g_{1-\Delta,1-J}^{\text{pure}}(\chi, \bar{\chi}) \frac{e^{-i\pi(a+b)}}{\kappa_{J+\Delta}} \end{aligned} \quad (4.3.11)$$

where κ_β has been defined in (4.1.4) and a and b have been defined in (4.1.5).

Interchanging χ and $\bar{\chi}$ followed leads to the following change to the pure conformal block:

$$g_{J,\Delta}^{\text{pure}}(\chi, \bar{\chi}) = g_{-J-d+2,\Delta}^{\text{pure}}(\bar{\chi}, \chi) \frac{e^{-i\pi \frac{d-2}{2}} \Gamma(-J - \frac{d-2}{2}) \Gamma(1 - J - \frac{d-2}{2})}{\Gamma(-J) \Gamma(3 - J - d)} \\ + g_{J,\Delta}(\bar{\chi}, \chi) \frac{e^{i\sin(\pi \frac{d-2}{2})}}{\sin(\pi(J + \frac{d-2}{2}))} \quad (4.3.12)$$

In order to get an analytic continuation of the pure conformal block $g(\chi, \bar{\chi})$ around $\chi = 1$ is given by acting on (4.3.11) with (4.3.12) in a conjugate manner, i.e apply (4.3.12), (4.3.11) and (4.3.12) in this particular order.

Once we have highlighted the behaviour of the pure conformal block under these 3 independent monodromies, we can move on to actually performing the analytic continuation in cross ratio space.

4.3.3 Analytic Continuation

In this section we will finally perform the analytic continuation. We will require the comments made in the earlier subsections of the current section as we analytically continue parts of the integrand separately.

Change of Coordinates

We first change to "radial" and "angular" coordinates denoted by σ and ω respectively. They are defined as follows:

$$\rho = \sigma\omega \\ \bar{\rho} = \frac{\sigma}{\omega} \quad (4.3.13)$$

In these coordinates, the equation (4.2.1) converts into:

$$c(J, \Delta) = N(J, \Delta) \int_0^1 \sigma d\sigma \oint_{|\omega|=1} \frac{d\omega}{i\omega} \mu(\rho, \bar{\rho}) g(\rho, \bar{\rho}) F_{J,\Delta}(\rho, \bar{\rho}) \quad (4.3.14)$$

with $\mu(\rho, \bar{\rho})$ along with the Jacobian factors is given by:

$$\mu(\rho, \bar{\rho}) = \frac{(1-\rho)^2(1-\bar{\rho})^2}{16\rho^2\bar{\rho}^2} \left| \frac{(1-\rho\bar{\rho})(\rho-\bar{\rho})}{4\rho\bar{\rho}} \right|^{d-2} \left(\frac{(1-\rho)(1-\bar{\rho})}{(1+\rho)(1+\bar{\rho})} \right)^{2(a+b)} \quad (4.3.15)$$

Branch points and branch cuts

The points 1 and -1 correspond to the branch points of the measure factor $|\chi - \bar{\chi}|^{d-2}$. These can be integrated out and do not pose a threat to the kinematics of analytic continuation. The other branch points at $\omega = \pm\sigma$ and $\omega = \pm 1/\sigma$ correspond to the location where some configuration of points get lightlike separated.

- (1,4) and (2,3):

$$x_{14}^2 = x_{23}^2 = \left(1 - \frac{1}{\rho}\right)(\bar{\rho} - 1) \quad (4.3.16)$$

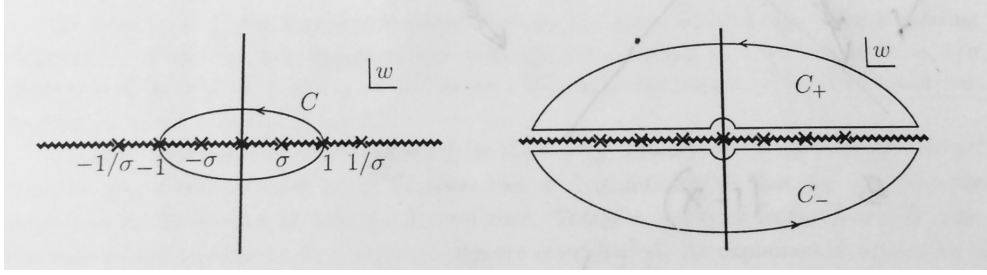


Figure 4.1: The figure shows the complex w plane - the branch points and the orientation of the branch cuts. 1 and -1 are present due to the measure factor and are integrable. So they are not as important as the other four. The positive branch points correspond to the t branch and the negative ones to the u branch. (Borrowed from [3]).

The configuration where $(4 > 1)$ and $(2 > 3)$ are timelike corresponds to the Lorentzian patch R_1 . To keep up with the notation borrowed from the Froissart-Gribov formalism, this configuration corresponds to the t channel contribution. We get the branch points when $x_{14}^2 = 0$. This implies in the σ, ω language as the following:

$$\begin{aligned}\rho &= \sigma \\ \bar{\rho} &= 1/\sigma\end{aligned}\tag{4.3.17}$$

- **(3,1) and (2,4):**

$$x_{24}^2 = x_{13}^2 = \left(1 + \frac{1}{\rho}\right)(\bar{\rho} + 1)\tag{4.3.18}$$

The configuration where $(3 > 1)$ and $(2 > 4)$ are timelike corresponds to the Lorentzian patch R_2 . To keep up with the notation borrowed from the Froissart-Gribov formalism, this configuration corresponds to the u channel contribution. We get the branch points when $x_{24}^2 = 0$. This implies in the σ, ω language as the following:

$$\begin{aligned}\omega &= \sigma \\ \omega &= -1/\sigma\end{aligned}\tag{4.3.19}$$

- **(1,2) or (3,4):** The locations where these pairs of points become light-like separated are given by:

$$\begin{aligned}\omega &= 0 \\ \omega &= \infty\end{aligned}\tag{4.3.20}$$

This situation corresponds to the Regge limit and this limit will be important when we deform our contour.

The figure (4.3.3) highlights the branch points and the corresponding orientation of the branch cuts. The figure is plotted after having fixed $\sigma < 1$.

Mapping kinematics in $\chi - \bar{\chi}$ plane to kinematics in ω plane

In this subsection, we will map out the kinematics in the $\chi - \bar{\chi}$ complex plane to kinematics in the ω plane. We will see how approaching σ from the right in (4.3.3) leads to an anticlockwise rotation about $\bar{\chi} = 1$ and some other monodromies.

- **ω crosses σ :**

To see how this translates in the $\chi - \bar{\chi}$ plane, we follow the following ladder of logic. We first fix ω as follows.

$$\omega = \sigma + \delta + i\epsilon \quad (4.3.21)$$

This will help us to follow the kinematics depending on how we tune δ and ϵ . To see this:

$$\begin{aligned} \bar{\chi} &= \frac{4\bar{\rho}}{(1+\bar{\rho})^2} \\ &= \frac{4\sigma\omega}{(\sigma+\omega)^2} \\ &= \frac{4\sigma^2 + 4\sigma(\delta + i\epsilon)}{4\sigma^2 \left(1 + \frac{\delta + i\epsilon}{2\sigma}\right)^2} \\ &= \left(1 + \frac{\delta}{\sigma} + i\frac{\epsilon}{\sigma}\right) \left(1 - \frac{\delta}{\sigma} - i\frac{\epsilon}{\sigma}\right) \\ &= 1 - \frac{\delta^2}{\sigma^2} + \frac{\epsilon^2}{\sigma^2} - \frac{2i\delta\epsilon}{\sigma^2} \end{aligned} \quad (4.3.22)$$

Therefore, as we move from a little to the right of σ to a little left of σ , we move from $\delta > 0$ to $\delta < 0$. This results in a change in the sign of the imaginary part. Also a variation in the δ value leads to initial increase in value of the real part till δ reaches 0 and then as δ decreases further, the value of the real part of $\bar{\chi}$ decreases. If we map these kinematics in the $\bar{\chi}$ plane, the branch point and branch cut structure of whose is given in the figure (3.3.7), we see that it corresponds to an anticlockwise rotation about $\bar{\chi} = 1$.

- **ω crosses $1/\sigma$:**

We will not go through the process again but if we follow a logic similar to the one outlined above, we see that this transition corresponds to an anticlockwise rotation about $\chi = 1$. This seems to make sense since the form of χ in terms of ω and σ is given by:

$$\chi = \frac{4\sigma\omega}{(1+\sigma\omega)^2} \quad (4.3.23)$$

Everything seems flipped in this case: σ to $1/\sigma$ and in the denominator $\sigma + \omega$ has given way to $\sigma\omega + 1$. Hence, it makes to arrive at the conclusion that making ω cross $1/\sigma$ from the right leads to an anticlockwise rotation about $\chi = 1$.

- **ω crosses 1:**

We will give a heuristic argument corresponding to this monodromy. Taking ω from greater than 1 to less than one is similar to taking a reciprocal.

When we defined the $\omega - \sigma$ variables, we said that the ω variable is similar to the angular variable. In complex analysis, when we take a reciprocal of the angular variable, we perform a complex conjugation. This is exactly what happens with this monodromy. We move from χ to $\bar{c}\bar{h}i$ and vice-versa.

- **ω crosses $-1/\sigma$:**
This corresponds to a u channel transition. As we moved around $\chi = 1$ for its t channel analog, here we move around $\chi = -\infty$ in an anticlockwise manner. Deriving this will mirror the steps we followed in (4.3.22).
- **ω crosses $-1/\sigma$:**
This corresponds to a u channel transition. As we moved around $\bar{\chi} = 1$ for its t channel analogue, here we move around $\bar{\chi} = -\infty$ in an anticlockwise manner. Deriving this will mirror the steps we followed in (4.3.22).

These are the three monodromies that are important to be noted before we perform the analytic continuation of the integral (4.3.14). In the next subsection, we finally get to the nitty-gritties of performing the analytic continuation.

Contour manipulations and monodromies

In the Euclidean version of the integral, we need to perform a contour integration along C in figure (4.3.3). As is evident from the $i\epsilon$ prescription from the analysis done in section (3.3.40) and detailed in appendix (A), moving to Lorentzian spacetime refers to the contour hugging the branch cut, i.e the contour has to be deformed so that the imaginary part tends to zero and we approach real time. To this end, we need to deform C in such a way so that, the deformed contour hugs the branch cuts, the orientation of whose is detailed in the figure (4.3.3). As we said in (4.3.2), it is better to express the conformal blocks and hence the harmonic function in terms of solutions which behave as power laws in the $\omega \rightarrow \infty$ and $\omega \rightarrow 0$. We expect from section (4.3.2) that on analytic continuation the harmonic function $_{J,\Delta}$ will be a linear combination of the 8 independent solutions highlighted earlier. As we deform the contour we need the ω^J pieces to drop off at ∞ and the ω^{-J} piece to drop off at 0. Keeping this in mind, we need to break the integral into two pieces - the first behaving as ω^J at ∞ and the second behaving as ω^{-J} near the origin. For the first piece, we deform the contour as given in the figure (4.3.3) and for the second piece, we deform the contour as given in figure (4.3.3).

Before moving on, we will highlight the behaviour of the 8 independent solutions in the Regge limit $\omega \rightarrow 0$ and $\omega \rightarrow \infty$. Refer equation (4.3.8). This will be important in the upcoming analysis. In the equations above, we mention their behaviour - ω^J , ω^{-J} , ω^Δ or $\omega^{-\Delta}$. The notation used is (J, Δ) referring to

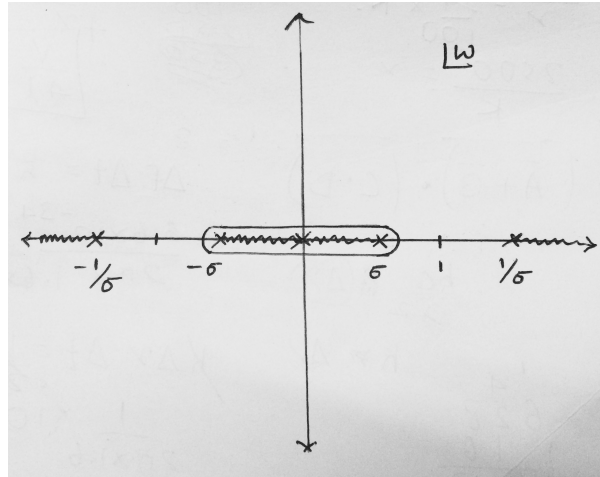


Figure 4.2: The figure shows the complex ω plane.

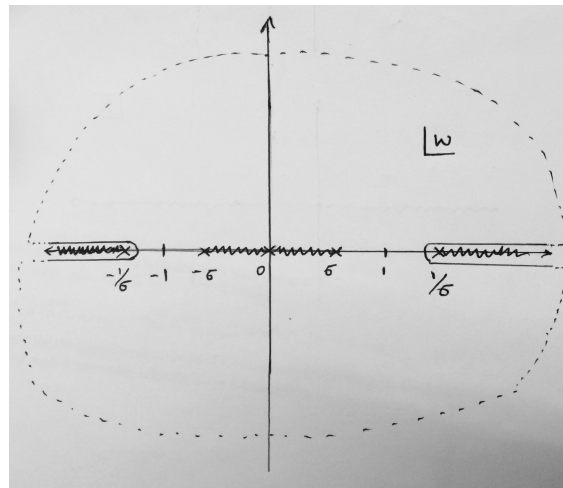


Figure 4.3: The figure shows the complex ω plane.

the pure conformal block $g_{J,\Delta}^{\text{pure}}$. Following are the equations for the limit $\omega \rightarrow 0$.

$$\begin{aligned}
(J, \Delta) &\rightarrow \omega^{-J} \\
(1 - \Delta, 1 - J) &\rightarrow \omega^{\Delta} \\
(-J - d + 2, \Delta) &\rightarrow \omega^J \\
(1 - \Delta, J + d - 1) &\rightarrow \omega^{\Delta} \\
(J, d - \Delta) &\rightarrow \omega^{-J} \\
(\Delta - d + 1, 1 - J) &\rightarrow \omega^{-\Delta} \\
(-J - d + 2, d - \Delta) &\rightarrow \omega^J \\
(\Delta - d + 1, J + d - 1) &\rightarrow \omega^{-\Delta}
\end{aligned} \tag{4.3.24}$$

And for the limit $\omega \rightarrow \infty$:

$$\begin{aligned}
(J, \Delta) &\rightarrow \omega^{-\Delta} \\
(1 - \Delta, 1 - J) &\rightarrow \omega^J \\
(-J - d + 2, \Delta) &\rightarrow \omega^{-\Delta} \\
(1 - \Delta, J + d - 1) &\rightarrow \omega^{-J} \\
(J, d - \Delta) &\rightarrow \omega^{\Delta} \\
(\Delta - d + 1, 1 - J) &\rightarrow \omega^J \\
(-J - d + 2, d - \Delta) &\rightarrow \omega^{\Delta} \\
(\Delta - d + 1, J + d - 1) &\rightarrow \omega^{-J}
\end{aligned} \tag{4.3.25}$$

As given in (4.1.3) and (4.3.10), we get the following expression for the harmonic function $F_{J,\Delta}$ in terms of the pure conformal block:

$$2F_{J,\Delta} = g_{J,\Delta}^{\text{pure}} + Bg_{-J-d+2,\Delta}^{\text{pure}} + Ag_{J,d-\Delta}^{\text{pure}} + ABg_{-J-d+2,d-\Delta}^{\text{pure}} \tag{4.3.26}$$

where

$$\begin{aligned}
A &= \frac{K_{J,d-\Delta}}{K_{J,\Delta}} \\
B &= \frac{\Gamma(J+d-2)\Gamma(-J-\frac{d-2}{2})}{\Gamma(J+\frac{d-2}{2})\Gamma(-J)}
\end{aligned} \tag{4.3.27}$$

We wish to change the contour so that it hugs the branch cuts, i.e the arcs at infinity and near the origin need to vanish. When we analytically continue, we will encounter scenarios highlighted in the earlier subsection (4.3.3). The analytically continued version of $F_{J,\Delta}$ would be then a linear combination of the 8 solutions given in (4.3.24). The monodromies classify the kinematics into four distinct regions : $(0, r)$, $(r, 1)$, $(1, 1/r)$ and $(1/r, \infty)$. We are only considering the t channel right now. So we consider only the positive real axis part. Refer (4.3.3) and (4.3.3). We will give a heuristic argument as to how we get the conformal block $G_{\Delta+1-d, J+d-1}$ at the end of the analytic continuation for each of the four regions shown above. We will detail the steps of the calculation for the $(0, r)$ region.

A Heuristic argument:

If we refer to figure (4.3.3), and focus our attention on the part of the contour above the real axis and stretching in the region $(0, \dots)$, we see that it crosses σ before touching the real axis again. This corresponds to crossing σ which translates to an anticlockwise rotation about $\bar{\chi} = 1$. Therefore we resort to the formula (4.3.11) for performing the analytic continuation. Now, as mentioned at the beginning of the section, we need to just isolate the parts that behave as ω^J near the origin. The way to think about this is that in the Euclidean theory itself we write down the harmonic function as a linear combination of the 8 independent solutions with the coefficients of the 6 extra solutions being zero. Then depending on the region one is in, we can perform the corresponding monodromy to analytically continue the formula. What this monodromy will essentially do is change these parameters which have been set to zero. So depending on the monodromy the appropriate pieces can be isolated in the appropriate regions. Therefore, in this case the pure conformal blocks $(-J-d+2, \Delta)$ and $(-J-d+2, d-\Delta)$ are the two pieces which behave as ω^J near the origin. However, we cannot just use these two blocks for isolation. We need to use the blocks we get by analytically continuing these two blocks too. These extra blocks are $(1-\Delta, J+d-1)$ and $(\Delta-d+1, J+d-1)$. These extra blocks behave as ω^Δ and $\omega^{-\Delta}$ respectively near the origin. These two are also the blocks that behave as ω^{-J} in the limit $\omega \rightarrow \infty$. Therefore we have a total of 4 conformal blocks that will be integrated over the contour (above real axis, for points greater than 0) in (4.3.3).

We will now analyse the implications of these four conformal blocks. The conformal block $G_{\Delta+1-d, J+d-1}$, when analytically continued via (4.3.11), gives the following expression:

$$\begin{aligned} G^\odot = & C \cdot g_{\Delta-d+1, J+d-1}^{\text{pure}} + D \cdot g_{-J-d+2, d-\Delta}^{\text{pure}} \\ & + BC \cdot g_{1-\Delta, J+d-1}^{\text{pure}} + BD \cdot g_{-J-d+2, \Delta}^{\text{pure}} \end{aligned} \quad (4.3.28)$$

where

$$\begin{aligned} C = & \left[1 - 2i \frac{e^{-i\pi(a+b)}}{\sin(\pi(J+\Delta))} \sin\left(\pi\left(\frac{J+\Delta}{2} + a\right)\right) \sin\left(\pi\left(\frac{J+\Delta}{2} + b\right)\right) \right] \\ D = & -\frac{i}{\pi} \frac{e^{-i\pi(a+b)}}{\kappa_{J+\Delta}} \end{aligned} \quad (4.3.29)$$

The four blocks in the expansion of $G_{\Delta+1-d, J+d-1}$ under analytic continuation using (4.3.11), are the same four blocks we isolated for integration in the region $(0, r)$. Thus, $N(J, \Delta)F_{J, \Delta}$ in the integrand organises itself into the conformal block $G_{\Delta+1-d, J+d-1}$.

A similar analysis will hold for the contour (4.3.3). The conformal blocks $(1-\Delta, J+d-1)$ and $(\Delta-d+1, J+d-1)$ behave as ω^{-J} near infinity and hence the arcs at infinity can be cut out. With these two, we have to add the analytical continuations of the blocks. These are precisely $(-J-d+2, \Delta)$ and $(-J-d+2, d-\Delta)$ which behave as $\omega^{-\Delta}$ and ω^Δ near infinity and as ω^J near the origin. These four blocks again combine to form the conformal block $G_{\Delta+1-d, J+d-1}$.

We will not detail the calculations for the remaining two regions. We will just mention the results. It turns out, after using all the monodromies, in all

the 4 regions of the t channel we highlighted that $N(J, \Delta)F_{J, \Delta}$ organises itself into the conformal block $G_{\Delta+1-d, J+d-1}$. Therefore, for all the regions on the positive real axis, we have the same contribution on analytically continuing $N(J, \Delta)F_{J, \Delta}$ - the conformal block $G_{\Delta+1-d, J+d-1}$. Now focus on the part we had considered at the very beginning of this chapter - $g(\rho, \bar{\rho})$. Depending on the rotation in the complex $\chi - \bar{\chi}$ plane, we had got a double commutator from this term. The four regions in the t channel provide all the requisite kinematics necessary to produce the double commutator. Also, since the conformal block $G_{\Delta+1-d, J+d-1}$, appears in each region, we get the final contribution from the t channel to be :

$$c(J, \Delta) = c^t(J, \Delta) + \text{u channel}$$

$$c^t(J, \Delta) = \frac{\kappa_{J+\Delta}}{4} \int_0^1 d\bar{\chi} \mu(\chi, \bar{\chi}) G_{\Delta+1-d, J+d-1}(\chi, \bar{\chi}) \text{dDisc}[g(\chi, \bar{\chi})] \quad (4.3.30)$$

For the u cut, as we did in the equation (1.0.2), the variables have a negative value, there exists an extra $(-1)^J$ factor. Note that, in this case, the rotation is about $\bar{\chi} = \infty$. The final inversion formula is given by adding up the contributions from the t and the u channels. The Lorentzian inversion formula is thus given by:

$$c(J, \Delta) = c^t(J, \Delta) + (-1)^J c^u(J, \Delta) \quad (4.3.31)$$

Thus we have achieved our goal of getting a formula for calculating the CFT parameters from the knowledge of the conformal block.

Aliter

In this section, we will go about the process of analytic continuation by following the method Caron-Huot presented in [3]. Again we will work primarily for the t channel and extend our results to the u channel. We have done most of the hard work in our previous presentation when we talked about getting the conformal block $G_{\Delta+1-d, J+d-1}$. To the main integral (4.3.14), we add zero in the form of a contour integral over a region with no poles. The blocks chosen as the integrands are the ones which vanish at ∞ , because we wish to get rid of the arcs at infinity. There are specifically two blocks which vanish at infinity $g_{\Delta+1-d, J+d-1}^{\text{pure}}$ and $g_{1-\Delta, J+d-1}^{\text{pure}}$.

$$c(J, \Delta) = N(J, \Delta) \int_0^1 \sigma d\sigma \oint_{|\omega|=1} \frac{d\omega}{i\omega} \mu(\rho, \bar{\rho}) g(\rho, \bar{\rho}) F_{J, \Delta}(\rho, \bar{\rho})$$

$$+ \int_0^1 \sigma d\sigma \sum_{\pm} \oint_{C_{\pm}} \frac{d\omega}{i\omega} \mu g e_{J, \Delta}^{\pm} \quad (4.3.32)$$

where

$$e_{J, \Delta}^{\pm}(\chi, \bar{\chi}) = e_{J, \Delta}^{\pm, 1} g_{\Delta+1-d, J+d-1}^{\text{pure}}(\bar{\chi}, \chi) + e_{J, \Delta}^{\pm, 2} g_{1-\Delta, J+d-1}^{\text{pure}}(\bar{\chi}, \chi) \quad (\omega \rightarrow \infty) \quad (4.3.33)$$

and $e_{J, \Delta}^{\pm, 1}$ and $e_{J, \Delta}^{\pm, 2}$ are constants for the contours above/below the branch cut corresponding to the pure conformal blocks $g_{\Delta+1-d, J+d-1}^{\text{pure}}$ and $g_{1-\Delta, J+d-1}^{\text{pure}}$. The second term is essentially zero. Refer figure (4.3.3) for the contours C_{\pm} . This extra term is to rid the expression of integrals over contours at infinity. To get

rid of the arcs at the origin, so that the contour actually hugs the branch cuts, we impose the following condition (for the contour above the branch cut):

$$N(J, \Delta) F_{J, \Delta} - e_{J, \Delta}^{+,1} g_{\Delta+1-d, J+d-1}^{\text{pure}} - e_{J, \Delta}^{+,2} g_{1-\Delta, J+d-1}^{\text{pure}} \propto \omega^J \quad (\omega \rightarrow 0 + i\epsilon) \quad (4.3.34)$$

To get the constants, we use the monodromies highlighted in (4.3.2). The above equation needs to be satisfied near the origin and the definition of $e_{J, \Delta}^{\pm}$ holds near $\omega \rightarrow \infty$. Therefore we use all three monodromies ω crossing $1/\sigma$, ω crossing 1 and finally ω crossing σ . Then we use the knowledge of 4.3.24, to isolate out the relevant blocks. This results in us getting the relevant conformal block $G_{\Delta+1-d, J+d-1}$ as the coefficients $e_{J, \Delta}^{\pm}$ turn out to be:

$$\begin{aligned} e_{J, \Delta}^{+,1} &= \frac{1}{4} \kappa_{J+\Delta} e^{i\pi(a+b+\frac{d-1}{2})} \\ e_{J, \Delta}^{+,2} &= e_{J, \Delta}^{+,1} \times \frac{\Gamma(\frac{d}{2} - \Delta) \Gamma(\Delta - 1)}{\Gamma(\Delta - \frac{d}{2}) \Gamma(d - \Delta - 1)} \end{aligned} \quad (4.3.35)$$

The appropriate factors cancel out and what we are left with is the familiar conformal block $G_{\Delta+1-d, J+d-1}$. In the manner analogous to the earlier method, we find that the $g(\rho, \bar{\rho})$ analytically continues itself to the double discontinuity or the double commutator. This process is independent of the analytic continuation of the harmonic function block. Therefore, in this case also, if we account for the contribution from the u channel, the final answer turns out to be (4.3.31).

In the next section, we describe some differences between the spacetime and the cross ratio derivation of the Lorentzian Inversion formula.

4.4 Comparing spacetime derivation and Cross ratio derivation

In chapters (3) and (4), we have described the two relatively distinct approaches to getting the inversion formula. In this section, we will highlight briefly the similarities and the differences between the two approaches

Similarities

- The essence of the approach remains the same. We start by getting an Euclidean inversion formula. Then we get down to analytically continuing it to Lorentzian spacetime.
- The four point function in the Regge limit needs to be well behaved, i.e it should not diverge. This point was given semblance by the paper on the bound on chaos [14].

Differences

- The main difference is the complex plane we choose to perform an analytical continuation in. For the spacetime derivation, we performed analytical continuation in the complex spacetime plane (lightcone coordinates). On the other hand, in the cross ratio derivation, we resorted to deforming the contours in the complex angular coordinate ω plane.

- A second difference is the presentation of the final formula. The CFT data is encoded in $I_{\Delta,J}$ in the spacetime derivation. On the other hand, for the cross ratio derivation, $c(J, \Delta)$ is the data we solve for. These are related by:

$$c(J, \Delta) = \frac{I_{\Delta,J}}{n_{\Delta,J}} K_{\Delta,J}^{\Delta_3, \Delta_4} \quad (4.4.1)$$

where $n_{\Delta,J}$ has been defined in (2.5.2) and $K_{\Delta,J}^{\Delta_3, \Delta_4}$ has been defined in (2.4.5).

In the next chapter, we summarise our results, and point towards the future directions this project could take us.

Chapter 5

Conclusion

In this report, we have presented the two derivations of the Lorentzian inversion formula: the spacetime derivation described in chapter 3, given by [22] and the cross ratio derivation described in chapter 4, given by [3]. There are a number of assumptions that have been made pertaining to the validity of the formula. These assumptions have been highlighted in the report. One of the most important points to be noted is the behaviour of the four point function in the Regge limit. The four point correlator has to be well behaved in the Regge limit for the derivation to be valid. As mentioned before, [14], offers a bound on the behaviour of the correlator, which makes this process valid. To this end, [14] and the inversion formula have introduced new questions in the field and a possibility of resolving existing issues through a new perspective. In fact, it is quite amazing to see that a physical result could be obtained from a complex analysis exercise. The exact physical nature of the derivation still remains hazy and is worth thinking about.

One of the important directions in which one could move forward is to generalise the formula to the case where the external operators would have spin. This has been documented in [12] through the formalism of light ray transforms. Briefly speaking, in this paper, the authors have tried to come up with a Lorentz invariant integral transform which generalise the shadow transform we talked about in chapter 2. What these special integral transforms do is that they convert the spinning correlators to the scalar case by integrating by parts with conformally covariant operators. This generalisation is used to derive the inversion formula we have talked about and its extension to external operators having spin. Another direction, along these lines would be generate a method for getting a formula for higher point correlators - maybe a general formula which in the four point correlator case boils down to the OPE inversion formula.

One more area where this could be used is in large N Chern Simons matter theories. The relation between four point functions in these theories manifests some new complications as compared to a correlator of four identical scalar operators. The following two theorems hold:

Theorem 1: In a CFT, the four point correlator G of identical scalars is completely fixed by its double discontinuity.

Theorem 2: In a large N CFT, the planar four point function G of identical scalars is fixed by its double discontinuity upto a function which is a sum of three contact AdS Witten diagrams with arbitrary coefficients.

Due to this difference, if we wish to calculate four point functions of double trace operators in large N theories, we run into problems. Studying how exactly these two connect together would be good exercise for stage two of our project. This calculation turns out to be non-trivial and is not as straightforward as one would have envisaged given the inversion formula. Things have started to move in this direction in the research community. Most prominently, [23] has managed to calculate the four point correlators in CFTs with weakly broken high spin symmetry at arbitrary t'Hooft coupling. Also, most recently, [1] has presented a method of extending the bootstrap philosophy to large N Chern-Simons vector models.

The inversion formula has provided us with a very powerful mathematical construct with tremendous physical content. Many of the future directions I have pointed out above are research topics on which researchers are working on right now. The formula has given researchers the power to think from newer perspectives. The questions being asked are different and in some cases decisive and definitive. As things stand, it can be safely said that the inversion formula is just a start. There exists many things still unexplained by the formula or remain unanswered due to lack of extensions of the theorem. Exploring options to expand its domain of applicability might lead to even more interesting consequences. It is theorems and formulae like the inversion formula which lend this field a sense of novelty, surprise and wonder - an element of strong intuition under the guise of serendipity which makes the journey in this field an adventure.

Chapter 6

Acknowledgements

I would like to thank Dr. Shiraz Minwalla for giving me an opportunity to work on a research project with him. The insightful discussions with him helped me get a new perspective of handling problems in research. The bootstrap seminars also served as a base and a primer, which helped me in getting motivated towards the topic even more. I would also like to thank Dr. Urjit Yajnik for the discussions, support and guidance over the course of these four months. I would also like to express my gratitude to Dr. Abhijit Gadde for resolving the questions I had during the course of this project. Thanks are also due to Indranil, Naveen and Shubham for helping me understand the topic better and for helping me out with some of the calculations. I would like to specially thank the Department of Theoretical Physics, Tata Institute of Fundamental Research for providing me with the resources and the perfect environment to pursue research. I have thoroughly enjoyed the B.Tech project - Stage 1 experience and hope to continue enjoying in the next semester, and for this I would like to express my heartfelt gratitude to the Department of Physics, Indian Institute of Technology, Bombay - for giving me the flexibility to pursue my passion and my interests in my final year of undergraduate studies.

Appendices

Appendix A

Wick rotation of correlators

In this appendix, we will give a brief look as to how different orderings in Lorentzian space correspond to the different paths taken in the complex plane so as to analytically continue our theory from Euclidean to Lorentzian spacetime. A detailed exposition of this discussion can be found in [8].

A.1 Analytic continuation

If we have a theory that has been described in Euclidean theory, we can translate the theory to a Lorentzian theory by performing a Wick's rotation. In the Euclidean theory, the metric is of the form

$$ds^2 = dx^2 + d\tau^2 \quad (\text{A.1.1})$$

where τ is the Euclidean time. If we perform the transformation :

$$\tau = it \quad (\text{A.1.2})$$

we get the Minkowski metric:

$$ds^2 = dx^2 - dt^2 \quad (\text{A.1.3})$$

where t refers to real time. We can imagine performing this transformation (A.1.2) in the complex τ plane where the real axis would correspond to the Euclidean time and the imaginary axis to real time.

A.2 Euclidean correlators are time ordered

Suppose we have a correlator in Euclidean theory. This correlator has to be time ordered. The reason lies in the definition of the correlator itself. Consider a two point function of two operators (in the Heisenberg definition):

$$\langle O_2(x_2, \tau_2) O_1(x_1, \tau_1) \rangle = \langle e^{-\tau_2 H} O_2(x_2, 0) e^{\tau_2 H} e^{-\tau_1 H} O_1(x_1, 0) e^{\tau_1 H} \rangle \quad (\text{A.2.1})$$

If we insert a complete basis of energy eigen kets we get a summation of the form :

$$e^{-(\tau_2 - \tau_1)H} = \sum_n e^{-(\tau_2 - \tau_1)E_n} \quad (\text{A.2.2})$$

This summation would be finite only if $\tau_2 > \tau_1$, i.e if the operators are time ordered.

A.3 Lorentzian correlators

Once we have a Euclidean correlator, which by definition is always time ordered, we can get Lorentzian correlators by performing a Wick's rotation. Now, depending on the path one takes in performing the transformation (A.1.2), in the complex plane, one can get Lorentzian correlators of various different time orderings. For a Lorentzian correlator, an operator in the Heisenberg picture transforms as:

$$O(x, t) = e^{iHt} O(x, 0) e^{-iHt} \quad (\text{A.3.1})$$

If we add a small imaginary component to each time coordinate of an operator in the Lorentzian correlator, then depending upon the ordering of these imaginary components, we can define a Lorentzian correlator of a particular time ordering. For instance, suppose we want to define the Lorentzian correlator :

$$\langle O_n(t_n) O_{n-1}(t_{n-1}) \dots O_2(t_2) O_1(t_1) \rangle \quad t_n \rightarrow t_n - i\epsilon_n \quad (\text{A.3.2})$$

We pick the following ordering of ϵ_i :

$$\epsilon_n > \epsilon_{n-1} > \dots > \epsilon_2 > \epsilon_1 \quad (\text{A.3.3})$$

This ordering defines the correlator (A.3.2) in Lorentzian space. We can see this by using (A.3.1) to expand inside the correlator as (A.2.2). Again, for maintaining the finiteness of the correlator, we need the exponent to be negative. This is given by ordering the imaginary parts of the real time as given in (A.3.3). This ordering of ϵ_i s is going to govern the ordering of operators in Lorentzian space. The ordering depends upon the path we take to perform the Wick transformation (A.1.2). The complex τ plane in which we perform the transformation can contain singularities pertaining to the branch points of the correlator. These singularities correspond to the case where the operators are inserted at space-like separated points. This is true specifically for conformal field theories due to the simple nature of the two point function - being dependent on just the distance between the two points. Now, across a branch cut corresponding to a branch point, one can have different operator orderings depending upon the ordering of ϵ_i s. We will give a very brief explanation of these orderings for the two points function.

A.4 An example

Consider the two point function in a conformal field theory. As was given in chapter (2) of this report, the two point function in Euclidean theory is given by:

$$\langle O(x, \tau) O(0, 0) \rangle = \frac{1}{(x^2 + \tau^2)^\Delta} \quad (\text{A.4.1})$$

We want to perform a continuous transformation from the real axis to the imaginary plane as mentioned in the figure A.1. Therefore, we define:

$$t = \tau e^{-i\phi} \quad (\text{A.4.2})$$

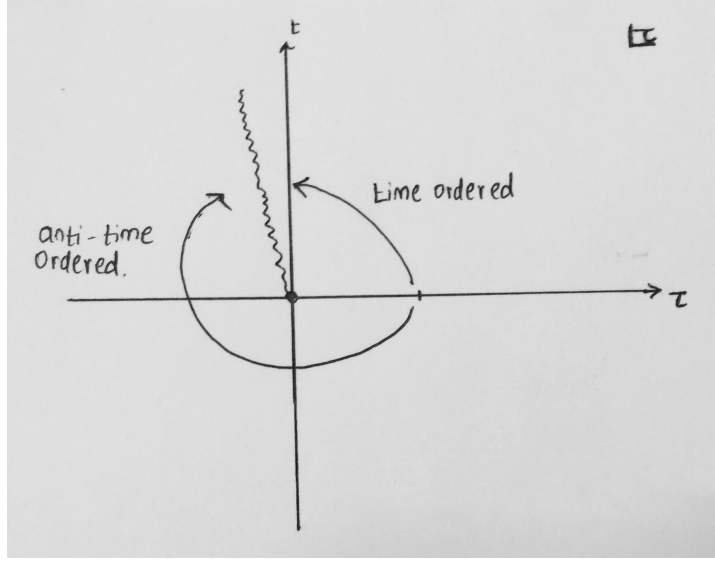


Figure A.1: We have taken the operator insertions at $(0, \tau)$ and $(0, 0)$. The time ordered and the anti-time ordered contours have been mentioned. For the time ordered contour, we do not cross any branch cuts and the points are time-like separated. The points are space-like separated in the anti time ordered case. Note the location of the branch cut and the branch point (point where the two points become light-like separated)

where the real time is defined as the t at which $\phi = \pi/2$ (follows from eq (A.1.2)). Therefore, we get the following:

$$\begin{aligned} \frac{1}{(x^2 + \tau^2)^\Delta} &= \frac{1}{(x^2 + t^2 e^{i2\phi})^\Delta} \\ &= \exp[-\Delta \log(x^2 + t^2 e^{i2\phi})] \end{aligned} \quad (\text{A.4.3})$$

Notice the location of the branch point and the orientation of the branch cut in the figure A.1. As mentioned earlier, the branch point corresponds to the point in the complex plane where (x, t) becomes light-like separated from the origin. We have chosen the branch cut such that it hugs the imaginary axis in the complex plane. Also, the logarithmic function has a branch cut at the same location. Therefore, depending on the choice of ϕ we will either be to the left of the branch cut or to the right of it. Depending on this, we will have an $i\pi$ or a $-i\pi$ contribution from the logarithmic function. Secondly, the choice of ϕ being to the left or right of the branch cut corresponds to the sign of ϕ . If we take the domain to be $(-\pi, \pi]$ then right of the branch cut corresponds to $-\phi$ and left corresponds to $+\phi$. Thus, since the sign of ϕ changes about a discontinuity, the ordering of operators in Lorentzian space changes. In A.1, we have highlighted the contours which correspond to the time ordered correlator and the anti-time ordered correlator.

We can see that ordering of operators in Lorentzian spacetime requires a choice of path taken to move from the Euclidean space. The presence of branch points and the branch cuts causes a choice in ordering. If we cross a branch cut,

the ordering changes. Crossing a branch cut corresponds to the two operators being time-like separated. If we do not cross one, then these points are space-like separated. For higher point functions, the number of such branch points will increase, causing the paths to be more complicated. However, the essence of the ordering as outlined above will remain the same.

Bibliography

- [1] Ofer Aharony, Luis F. Alday, Agnese Bissi, and Ran Yacoby. “The Analytic Bootstrap for Large N Chern-Simons Vector Models”. In: *JHEP* 08 (2018), p. 166. DOI: [10.1007/JHEP08\(2018\)166](https://doi.org/10.1007/JHEP08(2018)166). arXiv: [1805.04377 \[hep-th\]](https://arxiv.org/abs/1805.04377).
- [2] R. Blumenhagen and E. Plauschinn. *Introduction to Conformal Field Theory: With Applications to String Theory*. Lecture Notes in Physics. Springer Berlin Heidelberg, 2009. ISBN: 9783642004490. URL: <https://books.google.co.in/books?id=UmWvBSnyg0oC>.
- [3] Simon Caron-Huot. “Analyticity in Spin in Conformal Theories”. In: *JHEP* 09 (2017), p. 078. DOI: [10.1007/JHEP09\(2017\)078](https://doi.org/10.1007/JHEP09(2017)078). arXiv: [1703.00278 \[hep-th\]](https://arxiv.org/abs/1703.00278).
- [4] Miguel S. Costa, Vasco Goncalves, and Joao Penedones. “Conformal Regge theory”. In: *JHEP* 12 (2012), p. 091. DOI: [10.1007/JHEP12\(2012\)091](https://doi.org/10.1007/JHEP12(2012)091). arXiv: [1209.4355 \[hep-th\]](https://arxiv.org/abs/1209.4355).
- [5] V.K. Dobrev, G. Mack, V.B. Petkova, S.G. Petrova, and I.T. Todorov. *Harmonic Analysis: On the n -Dimensional Lorentz Group and Its Application to Conformal Quantum Field Theory*. Lecture Notes in Physics. Springer Berlin Heidelberg, 1977. ISBN: 9783540081500. URL: <https://books.google.co.in/books?id=XU2hQgAACAAJ>.
- [6] F. A. Dolan and H. Osborn. “Conformal four point functions and the operator product expansion”. In: *Nucl. Phys.* B599 (2001), pp. 459–496. DOI: [10.1016/S0550-3213\(01\)00013-X](https://doi.org/10.1016/S0550-3213(01)00013-X). arXiv: [hep-th/0011040 \[hep-th\]](https://arxiv.org/abs/hep-th/0011040).
- [7] P. Francesco, P. Di Francesco, P. Mathieu, D. Sénéchal, and D. Senechal. *Conformal Field Theory*. Graduate Texts in Contemporary Physics. Springer, 1997. ISBN: 9780387947853. URL: <https://books.google.co.in/books?id=keUrdME5rhIC>.
- [8] Thomas Hartman, Sachin Jain, and Sandipan Kundu. “Causality constraints in conformal field theory”. In: *Journal of High Energy Physics* 2016.5 (May 2016), p. 99. ISSN: 1029-8479. DOI: [10.1007/JHEP05\(2016\)099](https://doi.org/10.1007/JHEP05(2016)099). URL: [https://doi.org/10.1007/JHEP05\(2016\)099](https://doi.org/10.1007/JHEP05(2016)099).
- [9] Matthijs Hogervorst and Slava Rychkov. “Radial Coordinates for Conformal Blocks”. In: *Phys. Rev.* D87 (2013), p. 106004. DOI: [10.1103/PhysRevD.87.106004](https://doi.org/10.1103/PhysRevD.87.106004). arXiv: [1303.1111 \[hep-th\]](https://arxiv.org/abs/1303.1111).

- [10] Filip Kos, David Poland, and David Simmons-Duffin. “Bootstrapping mixed correlators in the 3D Ising model”. In: *Journal of High Energy Physics* 2014.11 (Nov. 2014), p. 109. ISSN: 1029-8479. DOI: [10.1007/JHEP11\(2014\)109](https://doi.org/10.1007/JHEP11(2014)109). URL: [https://doi.org/10.1007/JHEP11\(2014\)109](https://doi.org/10.1007/JHEP11(2014)109).
- [11] Filip Kos, David Poland, and David Simmons-Duffin. “Bootstrapping the $O(N)$ vector models”. In: *Journal of High Energy Physics* 2014.6 (June 2014), p. 91. DOI: [10.1007/JHEP06\(2014\)091](https://doi.org/10.1007/JHEP06(2014)091). URL: [https://doi.org/10.1007/JHEP06\(2014\)091](https://doi.org/10.1007/JHEP06(2014)091).
- [12] Petr Kravchuk and David Simmons-Duffin. “Light-ray operators in conformal field theory”. In: (2018), pp. 236–321. arXiv: [1805.00098 \[hep-th\]](https://arxiv.org/abs/1805.00098).
- [13] Hong Liu. *Relativistic Quantum Field Theory II, MIT OCW Lecture Notes, Lecture 5*. MIT Open Course Ware. 2010. URL: https://ocw.mit.edu/courses/physics/8-324-relativistic-quantum-field-theory-ii-fall-2010/lecture-notes/MIT8_324F10_Lecture5.pdf.
- [14] Juan Maldacena, Stephen H. Shenker, and Douglas Stanford. “A bound on chaos”. In: *Journal of High Energy Physics* 2016.8 (Aug. 2016), p. 106. ISSN: 1029-8479. DOI: [10.1007/JHEP08\(2016\)106](https://doi.org/10.1007/JHEP08(2016)106). URL: [https://doi.org/10.1007/JHEP08\(2016\)106](https://doi.org/10.1007/JHEP08(2016)106).
- [15] Hitoshi Murayama. *Faddeev Popov Ghosts*. 2007. URL: <http://hitoshi.berkeley.edu/230A/FPghosts.pdf>.
- [16] Joao Penedones. “TASI lectures on AdS/CFT”. In: *Proceedings, Theoretical Advanced Study Institute in Elementary Particle Physics: New Frontiers in Fields and Strings (TASI 2015): Boulder, CO, USA, June 1-26, 2015*. 2017, pp. 75–136. DOI: [10.1142/9789813149441_0002](https://arxiv.org/abs/1608.04948). arXiv: [1608.04948 \[hep-th\]](https://arxiv.org/abs/1608.04948).
- [17] David Poland and David Simmons-Duffin. “The conformal bootstrap”. In: *Nature Phys.* 12.6 (2016), pp. 535–539. DOI: [10.1038/nphys3761](https://doi.org/10.1038/nphys3761).
- [18] Slava Rychkov. *EPFL Lectures on Conformal Field Theory in $D=3$ Dimensions*. SpringerBriefs in Physics. 2016. ISBN: 9783319436258, 9783319436265. DOI: [10.1007/978-3-319-43626-5](https://doi.org/10.1007/978-3-319-43626-5). arXiv: [1601.05000 \[hep-th\]](https://arxiv.org/abs/1601.05000).
- [19] Slava Rychkov and Pierre Yvernay. “Remarks on the Convergence Properties of the Conformal Block Expansion”. In: *Phys. Lett. B* 753 (2016), pp. 682–686. DOI: [10.1016/j.physletb.2016.01.004](https://doi.org/10.1016/j.physletb.2016.01.004). arXiv: [1510.08486 \[hep-th\]](https://arxiv.org/abs/1510.08486).
- [20] David Simmons-Duffin. “Projectors, Shadows, and Conformal Blocks”. In: *JHEP* 04 (2014), p. 146. DOI: [10.1007/JHEP04\(2014\)146](https://doi.org/10.1007/JHEP04(2014)146). arXiv: [1204.3894 \[hep-th\]](https://arxiv.org/abs/1204.3894).
- [21] David Simmons-Duffin. “The Conformal Bootstrap”. In: *Proceedings, Theoretical Advanced Study Institute in Elementary Particle Physics: New Frontiers in Fields and Strings (TASI 2015): Boulder, CO, USA, June 1-26, 2015*. 2017, pp. 1–74. DOI: [10.1142/9789813149441_0001](https://arxiv.org/abs/1602.07982). arXiv: [1602.07982 \[hep-th\]](https://arxiv.org/abs/1602.07982).
- [22] David Simmons-Duffin, Douglas Stanford, and Edward Witten. “A space-time derivation of the Lorentzian OPE inversion formula”. In: *JHEP* 07 (2018), p. 085. DOI: [10.1007/JHEP07\(2018\)085](https://doi.org/10.1007/JHEP07(2018)085). arXiv: [1711.03816 \[hep-th\]](https://arxiv.org/abs/1711.03816).

- [23] Gustavo J. Turiaci and Alexander Zhiboedov. “Veneziano Amplitude of Vasiliev Theory”. In: *JHEP* 10 (2018), p. 034. DOI: [10.1007/JHEP10\(2018\)034](https://doi.org/10.1007/JHEP10(2018)034). arXiv: [1802.04390](https://arxiv.org/abs/1802.04390) [[hep-th](#)].